Autophagy inhibition enables Nrf2 to exaggerate the progression of diabetic cardiomyopathy in mice

Huimei Zang[1], Weiwei Wu[1], Lei Qi[1], Wenbin Tan[1], Prakash Nagarkatti[2], Mitzi Nagarkatti[2], Xuejun Wang[3], Taixing Cui[1].

[1]Department of Cell Biology and Anatomy, [2]Department of Pathology, Microbiology and Immunology, School of Medicine, University of South Carolina, Columbia, SC 29208, USA.

[3]Division of Basic Biomedical sciences, University of South Dakota Sanford School of Medicine, Vermillion, SD 57069, USA

A short running title: Nrf2-mediated progression of diabetic cardiomyopathy

Address correspondence: Dr. Taixing Cui, University of South Carolina School of Medicine, Tel: 803-216-3804; Email: taixing.cui@uscmed.sc.edu

ONLINE MATERIALS

I. Online Tables

II. Supplementary Figures and Figure Legends

I. Online Tables

Online Table 1. Antibody Information

Name	MW (kDa)	Characteristics	Sources
Anti-Nrf2	100	Rabbit polyclonal anti-Nrf2 **(WB)**	Proteintech Cat#: 16396-1-AP
Anti-LC3	14,16	Rabbit polyclonal anti-LC3 (**WB**)	Sigma-Aldrich Cat#: L8918
Anti-Atg5	56	Rabbit polyclonal anti-Atg5(C-terminal) (**WB**)	Sigma-Aldrich Cat#: A0731
Anti-Atg7	75	Rabbit polyclonal anti-Atg7 (**WB**)	Sigma-Aldrich Cat#: A2856
Anti-Atg16L1	66	Rabbit polyclonal anti-Atg16L1 (**WB**)	Sigma-Aldrich Cat#: SAB2103567
Anti-Beclin-1	60	Rabbit polyclonal anti-Beclin-1 (**WB**)	Sigma Aldrich Cat#: PRS3613
Anti-8OHdG	N/A	Mouse monoclonal anti-8OHdG(15A3) (**IHC**)	Santa Cruz Cat#: sc66036
Anti-beta Actin (βactin)	43	Mouse monoclonal anti-Beta actin (βactin) Clone AC-15	Sigma Aldrich Cat#: A1978
Anti-GAPDH	37	Mouse monoclonal anti-GAPDH Clone GAPDH-71.1 (**WB**)	Sigma-Aldrich Cat#: G8795
Anti-p62	62	Rabbit polyclonal anti-p62/SQSTM1 (**WB**)	Sigma Aldrich Cat#: P0067
Anti-4HNE	N/A	Mouse monoclonal anti-4 HNE (HNEJ-2) (**IHC**)	Abcam Cat#: ab48506
Anti-NQO1	28	Rabbit polyclonal anti-NQO1(C-terminal) (**WB**)	Sigma Aldrich Cat#: N5288

MW, predicted molecular weight; **IHC**, Immunohistochemistry staining; **WB**, Western blot analysis

Online Table 2. Primer information for qPCR

Primers	Gene access #	Forward (5'—3')	Reverse (5'—3')	Product
mouse				
Acsl4	NM_207625.2	AGAGTCCAAAGCGAGGGAGA	TCTCTCCAGTTCCCAAACGC	152
Agt	NM_007428.4	CGGAGGCAAATCTGAACAACAT	ACAAGGCCTCACACCACACTCT	250
Atg5	NM_001358596.1	GGTTCCGAGGGCGGAAGTGC	CGGTCGGGTTCTGTCTGCCG	134
Atg7	NM_001253717.1	GTTGAGCGGCGACAGCATTA	GGAAAGCCTCATGGCAGGAA	133
Atg12	NM_026217.3	CCACAGCCCATTTCTTTGTT	GAAACAGCCACCCCAGAG	145
Atg16L1	NM_001205392.1	GCAGCAAAGGAACCTCTACCT	AGTTGGGACTCTCACATCTTACC	201
Cd36	NM_001159557.1	CTAGCTGATTACTTCTGTGTACTGC	TACGTGGCCCGGTTCTAATTCA	183
Cox2	AF378830.1	AACCGAGTCGTTCTGCCAAT	ATTTAGTCGGCCTGGGATGG	123
Fgf21	NM_020013.4	GCATACCCCATCCCTGACTC	AGGTGGGCTTCAGTGTCTTG	101
Fpn1	NM_016917.2	CTCCAGTCATTGGCTGTGGT	TTTTACAGCCAGAGCAGGGG	110
Fsp1/Aifm2	NM_153779.2	CTTACAAGCCAGAGACTGACCA	AGGCCTGTCACTGAAGAGTC	167
Fth1	NM_010239.2	CTGGAACTGCACAAACTGGC	CTCTCATCACCGTGTCCCAG	200
Gapdh	NM_001289726.1	GCACAGTCAAGGCCGAGAAT	GCCTTCTCCATGGTGGTGAA	151
Gpx4	NM_001037741.4	CCTCTGCTGCAAGAGCCTCCC	CTTATCCAGGCAGACCATGTGC	144
Hamp1	NM_032541.2	CTTTGCACGGGGAAGAAAGC	GCAACAGATACCACACTGGGA	131
Ho1	NM_010442.2	TGACACCTGAGGTCAAGCAC	GTCTCTGCAGGGGCAGTATC	184
Klf9	NM_010638.5	GCCGCCTACATGGACTTCG	GGTCACCGTGTTCCTTGGT	139
Lamp1	NM_001317353.1	TAGTGCCCACATTCAGCATCTCCA	TCCTGCCAATGAGGTAGGCAATGA	282
Lamp2	NM_010685.4	GGTGCTGGTCTTTCAGGCTTGATT	ACCACCCAATCTAAGAGCAGGACT	198

NQO1	NM_008706.5	AGGGCAGAAGGGAATTGCTC	AAAGAGCTGGAGAGCCAACC	154
Nrf2	NM_010902.4	CCTAGGTCCTTGTTCCGCC	CTAGTCCGAGCAGCGGAGA	105
Rab9	NM_019773.2	AGGACGTCCAGTGTGTGTCT	GTGTGGAAGAGCTGGGAATCA	199
Rab7	NM_001293652.1	GGCCGGAGCTTTGACCATAA	AACAGAGACGTCCGATTCCG	105
TFR1	NM_011638.4	AAGTGACGTAGATCCAGAGGG	AGTACTAGGAAGCGCCTCTACA	136
Rat				
Acsl4	NM_053623.1	CTCTCCGGGAGCTTCCTTCC	GCGTGACAGAGCGATATGGA	196
Agt	NM_134432.2	GCTGGAGCTAAAGGACACACA	GATGTATACGCGGTCCCCAG	130
Atg5	NM_001014250.1	AGCCTCTCTTCTCGGGAACT	GTTTCCACTCTCCAGCCGAA	141
Cd36	NM_031561.2	GTACTCTCTCCTCGGATGGC	TGCTTTCTATGTGGCCTGGT	158
Chac1	NM_001173437.1	CAGACACAGCATCCCCATGT	TGTGGGTCAACGGAGAACAG	139
Cox2	S67722.1	TGACTTTGGCAGGCTGGATT	ACTGCACTTCTGGTACCGTG	139
Fsp1/Aifm2	NM_001139483.1	AAGCATTGGGCTTTGGGAGT	GCCCCAGTTAATCCCTGCAT	166
Fth1	NM_012848.2	CTTTGCAACTTCGTCGCTCC	GTCCTGGTGGTAGTTCTGGC	109
Ftl1	NM_022500.4	GCTCCATACTCCGGATCAGC	AGCCCAGAGAGAGGTAGGTG	127
Hamp1	NM_053469.1	TCTCCTGCTTCTCCTCCTGG	TCAGCAGCGCACTGTCATC	125
Gapdh	NM_017008.4	TCTCTGCTCCTCCCTGTTCT	TACGGCCAAATCCGTTCACA	104
Gpx4	NM_001039849.3	GGGGACGCTGCAGACAG	CGAGCTCTCCTCCTCCGA	106
Klf9	NM_057211.1	ATAACAACGCCACTCACGGG	ACCAAAAGGGGGCATTTCCA	113
NQO1	NM_017000.3	GGCATCCAATCCTCCACCC	AATCCCCCGAGGCTTGTCA	175
Nrf2	NM_031789.2	GGTTGCCCACATTCCCAAAC	GGCTGGGAATATCCAGGGC	116
TfR1	NM_022712.1	TGCTTCAGAGTGCTCCCTTG	ACTTGCCGAGCAAGGCTAAA	117

Online Table 3. Metabolic profile of type 1 diabetic mice. Type 1 diabetes (T1D) in female wild type FVB/N mice at age of 8~9 weeks was induced as described in "Research Design and Methods" Fasting blood glucose as well as non-fasting triglyceride and cholesterol were measured at indicated time points. *, $p < 0.05$ vs. time 0 in the same groups, #, $p < 0.05$ vs. 3 months in the same groups.

	Ctl (Veh)			T1D (STZ)		
Time (months)	0	3	6	0	3	6
(n)	(n=3)	(n=3)	(n=3)	(n=4)	(n=4)	(n=3)
Glucose (mmol/L)	4.9±0.5	4.8±0.8	5.3±0.9	5.1±0.5	23.3±1.9*	24.0±2.0*
HbA1C (%)	4.9±0.3	4.7±0.5	4.9±0.5	4.8±0.3	16.2±1.2*	16.7±1.3*
Triglyceride (mg/dl)	112.7±9.7	113.5±19.4	120.7±46.2	115.6±9.0	184.5±7.4*	258.3±7.2*,#
Cholesterol (mg/dl)	102.1±8.2	115.2±38.3	121.7±33.9	103.6±10.7	153.7±15.8*	222±14.3*,#

II. Supplementary Figures and Figure Legends

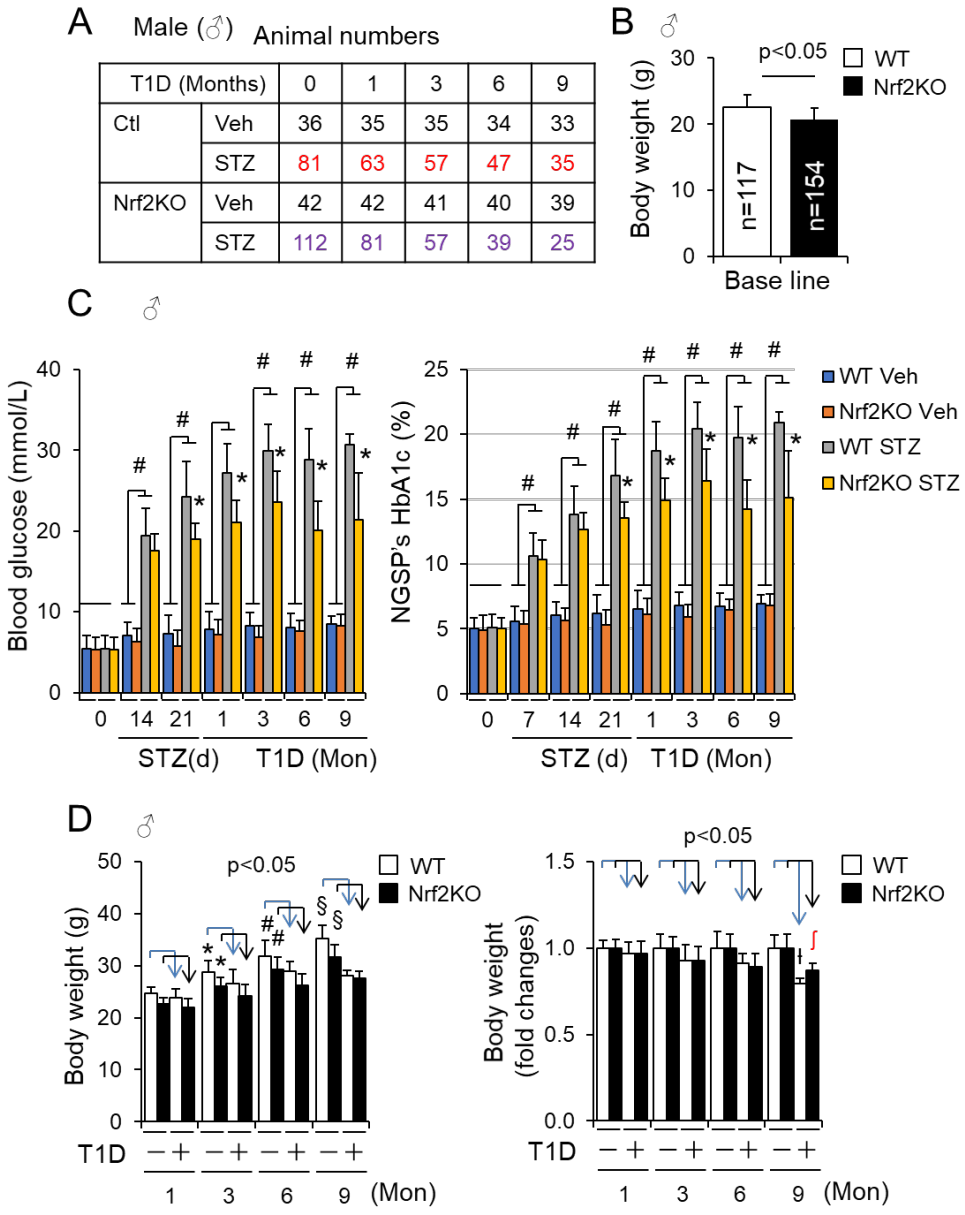

T1D (Months)		0	1	3	6	9
Ctl	Veh	36	35	35	34	33
	STZ	81	63	57	47	35
Nrf2KO	Veh	42	42	41	40	39
	STZ	112	81	57	39	25

Supplementary Fig. 1. The impact of global knockout of Nrf2 on STZ-induced type 1 diabetes in male mice. Type 1 diabetes (T1D) in adult littermates of male (♂) WT control (Ctl) and Nrf2KO mice in a C57BL/6J genetic background was induced by i.p. injection of STZ for 9 months (Mon) as described in "Research Design and Methods". *A*: Survived animal numbers of each group at each experimental end point. *B*: Body weights of WT and Nrf2KO mice at the basal condition. *C*: Fasting blood glucose levels and NGSP's HbA1c (%). * $p < 0.05$ vs. WT STZ groups. #, $p < 0.05$ between indicated groups at each end point. *D*: Body weight changes of WT and Nrf2KO mice after onset of T1D. Left panel shows arbitrary g and right panel shows fold changes. *, $p < 0.05$ vs. vehicle treated STZ (-) group at 1 Mon; #, $p < 0.05$ vs. vehicle treated

STZ (-) group at 3 Mon; §, $p < 0.05$ vs. vehicle treated STZ (-) group at 6 Mon; ɬ, $p < 0.05$ vs. STZ treated WT group at 6 Mon; ∫, $p < 0.05$ vs. STZ treated WT group at 9 Mon.

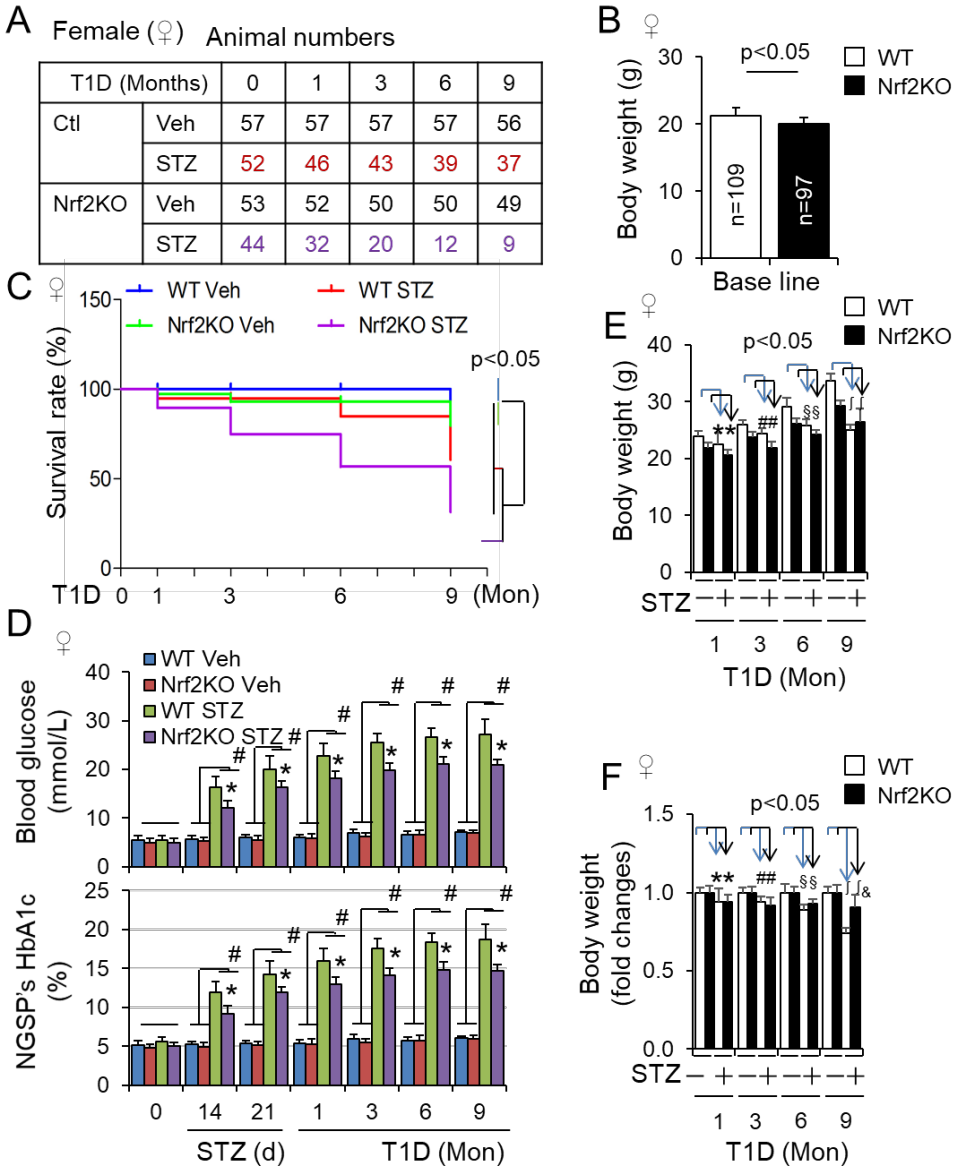

T1D (Months)		0	1	3	6	9
Ctl	Veh	57	57	57	57	56
	STZ	52	46	43	39	37
Nrf2KO	Veh	53	52	50	50	49
	STZ	44	32	20	12	9

Supplementary Fig. 2. The impact of global knockout of Nrf2 on STZ-induced type 1 diabetes in female mice. Type 1 diabetes (T1D) in adult littermates of female (♀) WT control (Ctl) and Nrf2KO mice in a C57BL/6J genetic background was induced by i.p. injection of STZ for 9 months (Mon) as described in "Research Design and Method". *A*: Survived animal numbers of each group at each experimental end point. *B*: Body weights WT and Nrf2KO mice at the basal condition. *C:* Kaplan Meier analysis of survival rates. *D*: Fasting blood glucose levels and NGSP's HbA1C (%). * $p < 0.05$ vs. WT STZ groups. #, $p < 0.05$ between indicated groups at each end point. *E, F*: Body weight changes (*E*, g) and (*F*, fold changes) of WT and Nrf2KO mice after onset of T1D. *, $p < 0.05$ vs. vehicle treated STZ (-) group at 1 Mon; #, $p < 0.05$ vs. STZ (-)

group (+) at 3 Mon; §, $p < 0.05$ vs. STZ (-) group at 6 Mon; ∫, $p < 0.05$ vs. STZ (-) groups at 6 Mon; &, $p < 0.05$ vs. STZ treated WT group at 9 Mon. Nrf2KO was confirmed by Western blot analysis using whole left ventricle (LV) tissue lysates at each end point (Supplementary Fig. 9*B*).

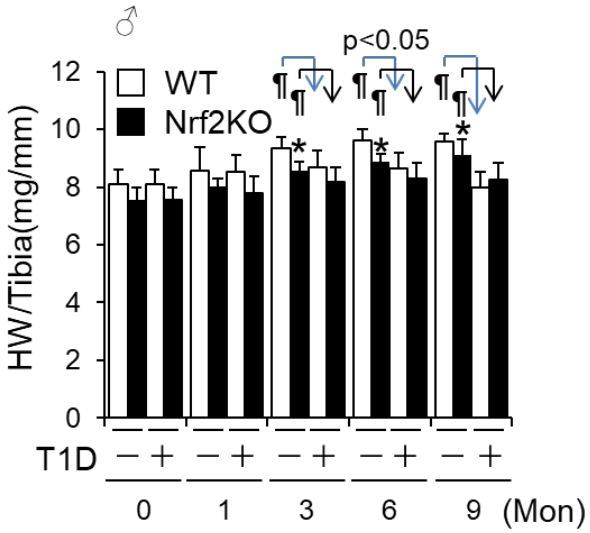

Supplementary Fig. 3. The impact of global knockout of Nrf2 on heart weight (mg) to tibia length (mm) ratios in STZ-induced diabetic male mice. Type 1 diabetes (T1D) was induced by i.p. injection of STZ in littermates of adult male (♂) WT and Nrf2KO mice in a C57BL/6J genetic background for 9 months (Mon) as described in "Research Design and Methods". Heat weight (HW in mg)/tibia length (Tibia in mm) ratios were quantified as described in "Research Design and Methods". #, $p < 0.05$ between indicated groups; *, $p < 0.05$ vs. WT STZ group at 9 Mon. Animal numbers for each group are indicated in Supplementary Fig. 1*A*

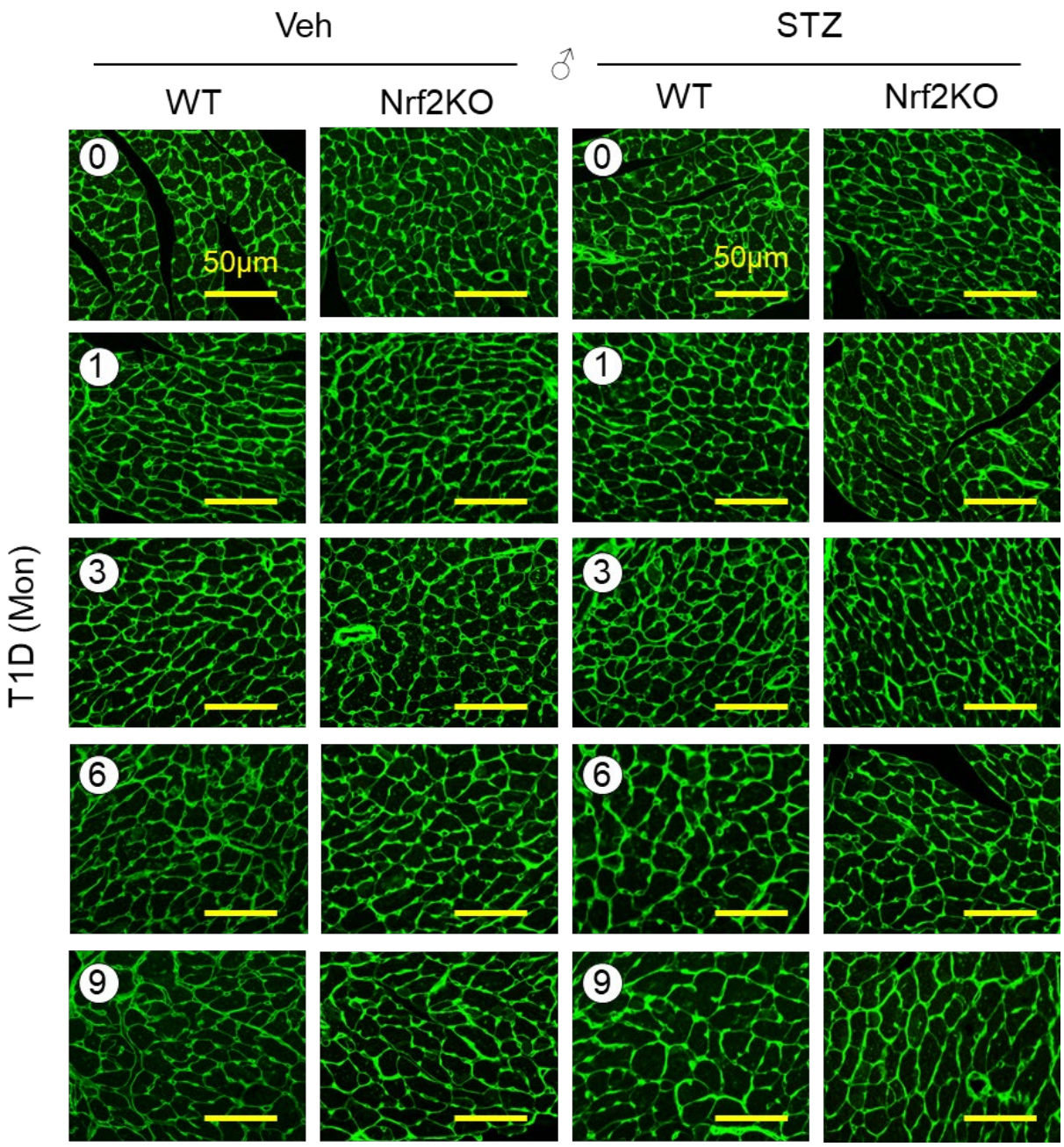

Supplementary Fig. 4. The impact of global knockout of Nrf2 on cardiomyocyte hypertrophy in STZ-induced type 1 diabetic male mice. Type 1 diabetes (T1D) was induced by i.p. injection of STZ in littermates of adult male (♂) WT and Nrf2KO mice in a C57BL/6J genetic background for 9 months (Mon) as described in "Research Design and Methods". Cardiomyocyte sizes were measured by Wheat Germ Agglutinin (WGA) staining in the left ventricle (LV) tissue sections of male (♂) littermates of WT and Nrf2KO mice at 0, 1, 3, 6, 9 months (Mon) after onset of STZ-induced type 1 diabetes (T1D). The results are representative WGA staining of Fig. 2*B*. Scale bar = 50 μm.

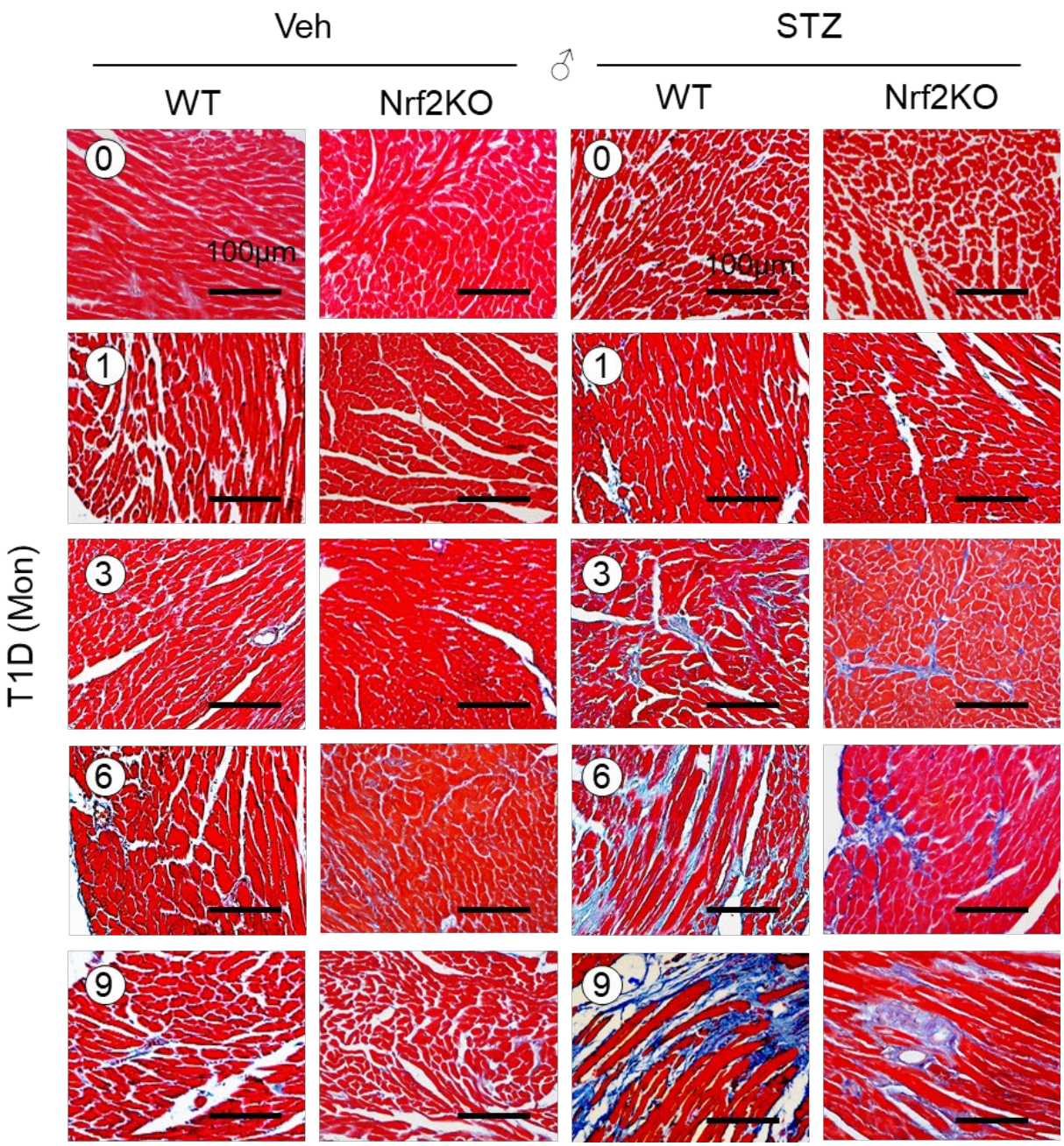

Supplementary Fig. 5. The impact of global knockout of Nrf2 on cardiac fibrosis in STZ-induced type 1 diabetic male mice. Type 1 diabetes (T1D) was induced by i.p. injection of STZ in littermates of adult male (♂) WT and Nrf2KO mice in a C57BL/6J genetic background for 9 months (Mon) as described in "Research Design and Methods". Cardiac fibrosis (%) was measured by Masson trichrome staining in in the left ventricle tissue (LV) sections of male (♂) littermates of WT and Nrf2KO mice at 0, 1, 3, 6, 9 months (Mon) after onset of STZ-induced type 1 diabetes (T1D). The results are representative Masson trichrome staining of Fig. 2*C*. Scale bar = 100 μm.

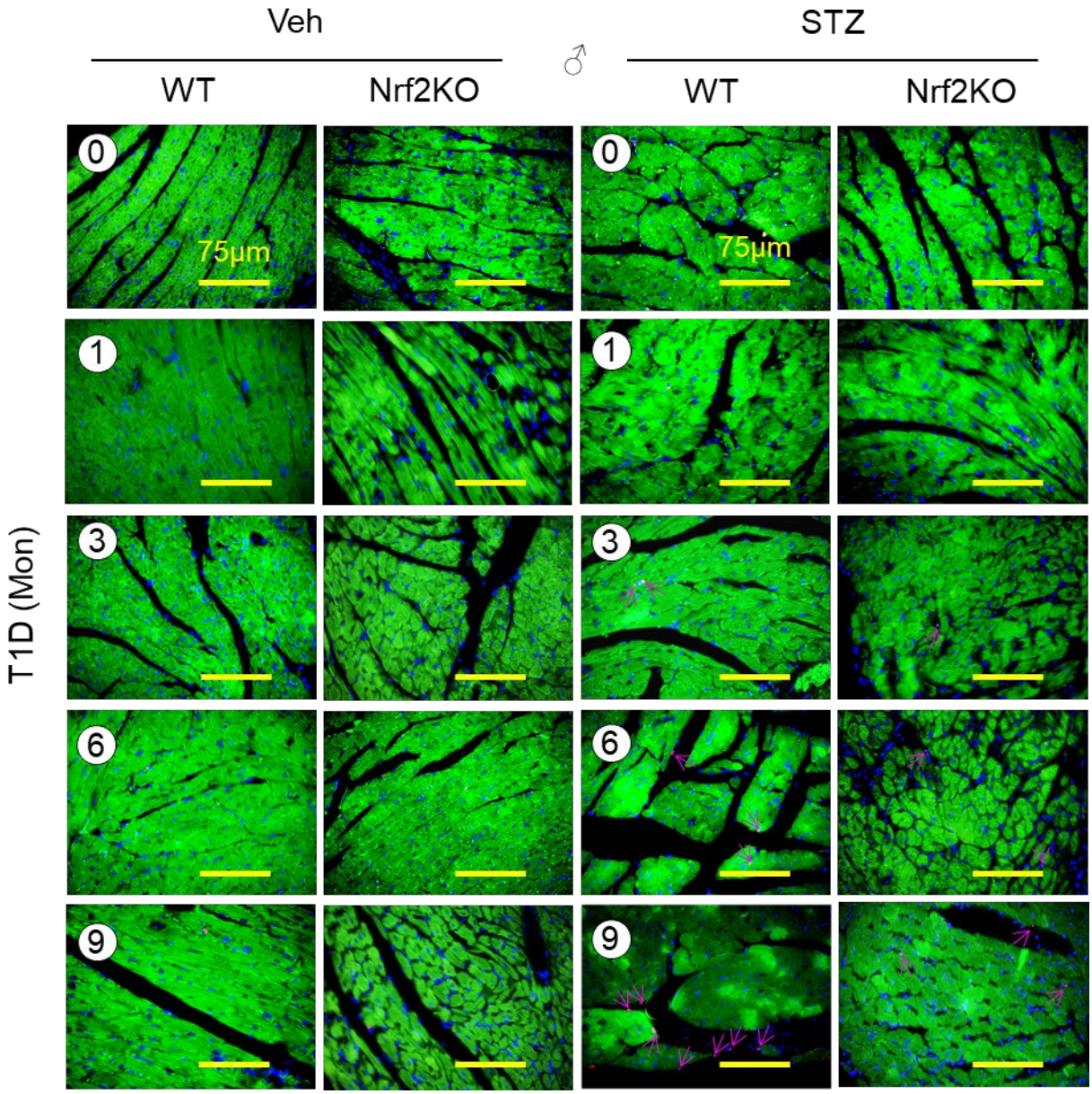

Supplementary Fig. 6. The impact of global knockout of Nrf2 on cardiac apoptosis in STZ-induced type 1 diabetic male mice. Type 1 diabetes (T1D) was induced by i.p. injection of STZ in littermates of adult male (♂) WT and Nrf2KO mice in a C57BL/6J genetic background for 9 months (Mon) as described in "Research Design and Methods". Cardiac apoptosis (%) was measured by Tunel staining in the left ventricle (LV) tissue sections of (♂) male littermates of WT and Nrf2KO mice at 0, 1, 3, 6, 9 months (Mon) after onset of STZ-induced type 1 diabetes (T1D). Cardiomyocytes (green) were marked by Alexa FluorTM 488 Phalloidin (Invitrogen A12379) binds F-actin. The results are representative Tunel staining of Fig. 2*D*. Scale bar = 75 μm.

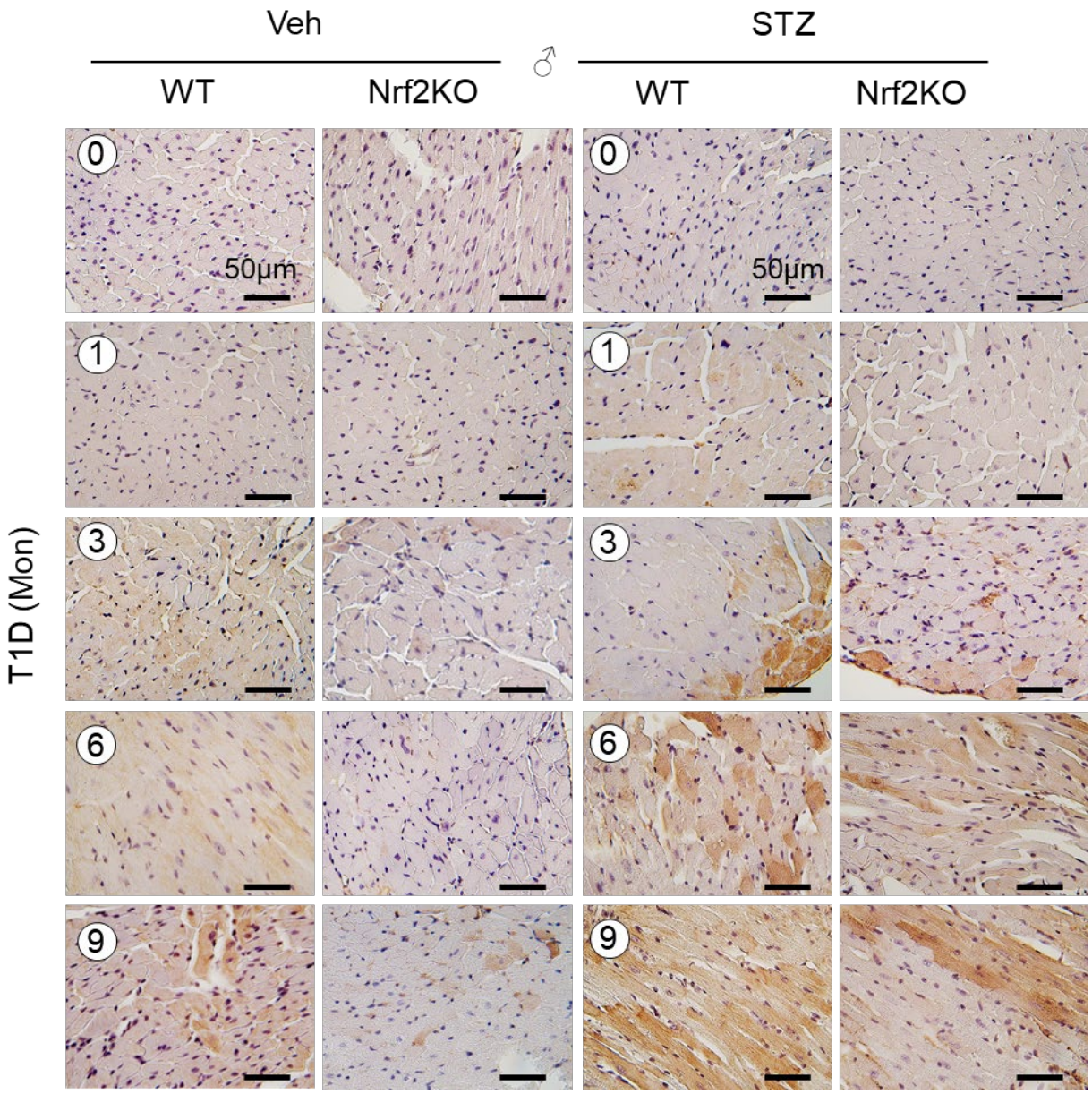

Supplementary Fig. 7. The impact of global knockout of Nrf2 on cardiac lipid peroxidation in STZ-induced type 1 diabetic male mice. Type 1 diabetes (T1D) was induced by i.p. injection of STZ in littermates of adult male (♂) WT and Nrf2KO mice in a C57BL/6J genetic background for 9 months (Mon) as described in "Research Design and Methods". Cardiac lipid peroxidation was assessed by quantifying the percentage of 4HNE positively stained areas in the left ventricle tissue (LV) sections of male (♂) littermates of WT and Nrf2KO mice at 0, 1, 3, 6, 9 months (Mon) after onset of STZ-induced type 1 diabetes (T1D). The results are representative 4HNE staining of Fig. 2*F*. Scale bar = 50 μm.

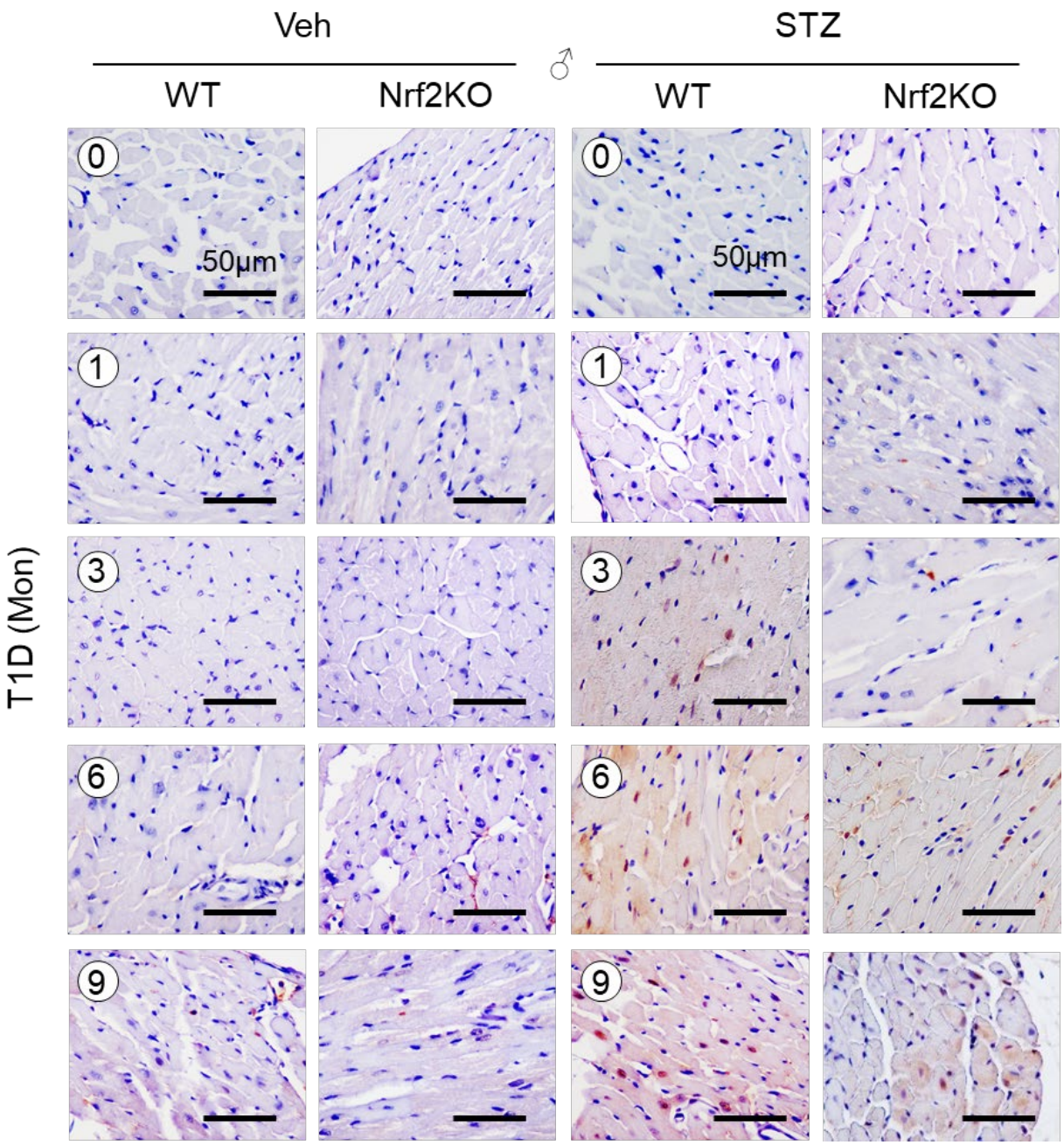

Supplementary Fig. 8. The impact of global knockout of Nrf2 on cardiac oxidative stress-induced DNA damage in STZ-induced type 1 diabetic male mice. Type 1 diabetes (T1D) was induced by i.p. injection of STZ in littermates of adult male (♂) WT and Nrf2KO mice in a C57BL/6J genetic background for 9 months (Mon) as described in "Research Design and Methods". Cardiac oxidative stress-induced DNA damage was assessed by quantifying the percentage of 8OHdG positively stained nuclei in the left ventricle (LV) tissue sections of male (♂) littermates of WT and Nrf2KO mice at 0, 1, 3, 6, 9 months (Mon) after onset of STZ-induced type 1 diabetes (T1D). The results are representative 8OHdG staining of Fig. 2*F*. Scale bar = 50 μm.

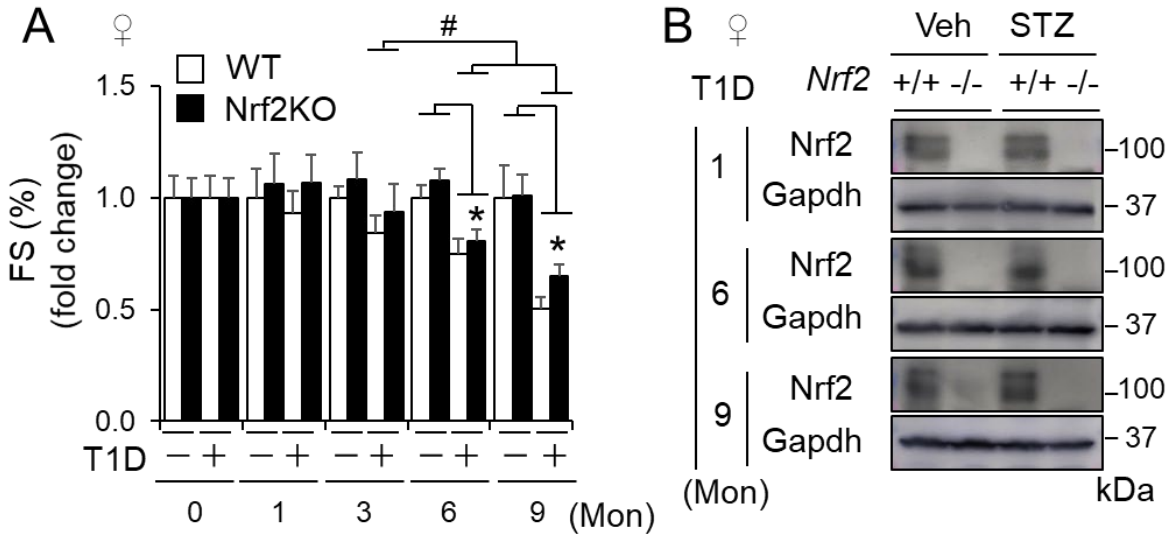

Supplementary Fig. 9. The impact of global knockout of Nrf2 on cardiac function in STZ-induced diabetic female mice. Type 1 diabetes (T1D) was induced by i.p. injection of STZ in littermates of adult female (♀) WT and Nrf2KO mice in a C57BL/6J genetic background for 9 months (Mon) as described in "Research Design and Methods". Animal numbers for each group are indicated in Supplementary Fig. 2*A*. *A*: FS (%). Cardiac function was monitored monthly by echocardiography. *, $p < 0.05$ vs. WT STZ group at each time point; #, $p < 0.05$ between indicated groups. *B*: Representative immunoblots of myocardial Nrf2 at each experimental end point. Western blot analysis was carried out using whole left ventricle (LV) tissue lysates of mice with indicated genotypes. WT, Nrf2+/+; Nrf2KO, Nrf2-/-.

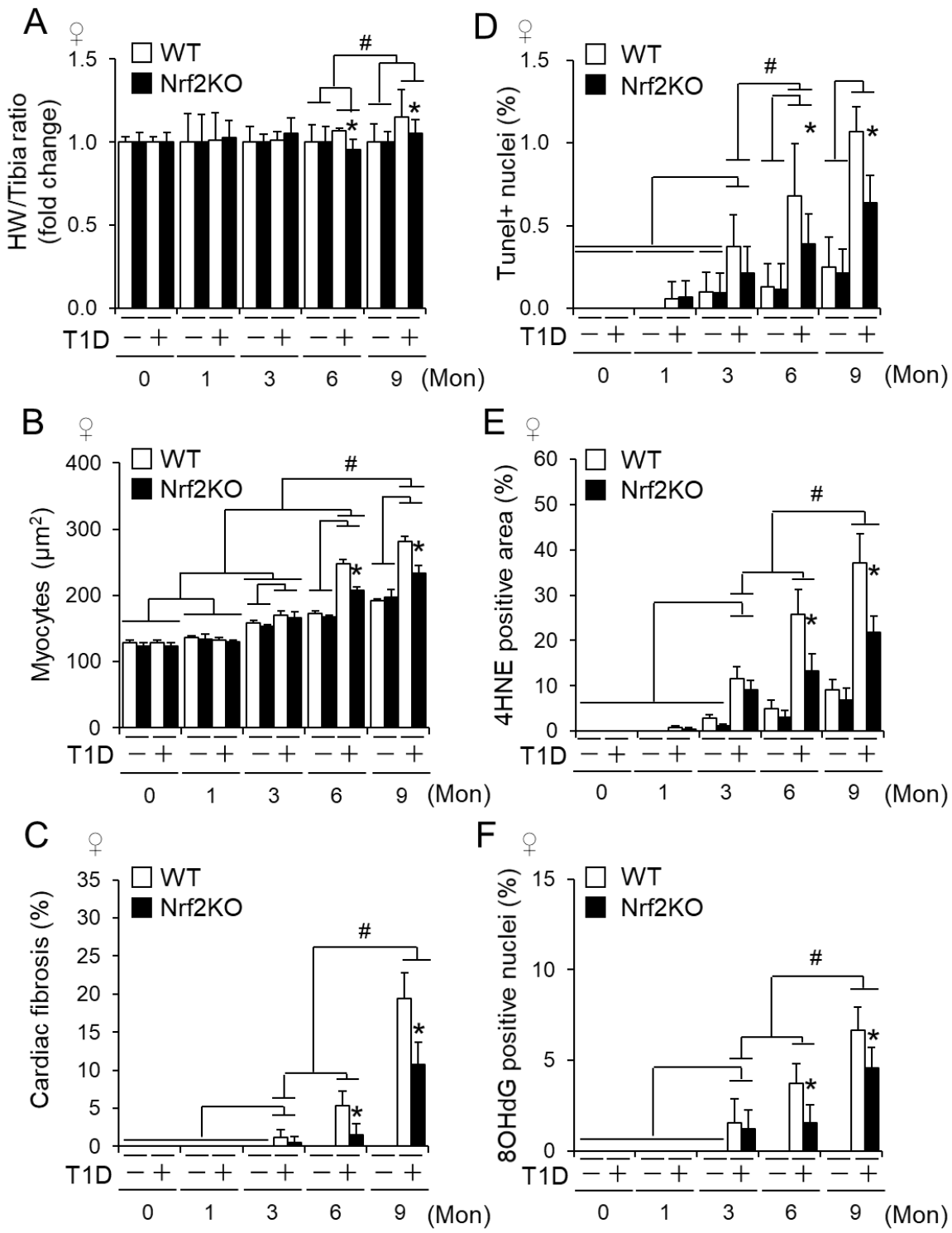

Supplementary Fig. 10. The impact of global knockout of Nrf2 on cardiac remodeling, cell death and oxidative stress in STZ-induced type 1 diabetic female mice. Type 1 diabetes (T1D) in adult littermates of female (♀) WT and Nrf2KO mice in a C57BL/6J genetic background was induced by i.p. injection of STZ for 9 months (Mon) and T1D-induced cardiomyopathy was assessed as described in "Research Design and Methods". *A*: Heat weight

(HW)/Tibia length ratio in fold changes. The values of vehicle treated groups are set as 1-fold. Animal numbers for each group are indicated in Supplementary Fig. 2*A*. *B*: Myocyte sizes. *C*: Cardiac fibrosis (%). *D*: Cardiac apoptosis. *E*: & *F*: Cardiac oxidative stress. *B-F* in left ventricle (LV) tissue sections of the WT and Nrf2KO mice (♀) with indicated treatments were analyzed. *B-F*: Animal numbers for each group are 6-8. *B-F*: #, $p < 0.05$ between indicated groups; *, $p < 0.05$ vs. STZ treated WT groups at the same end points.

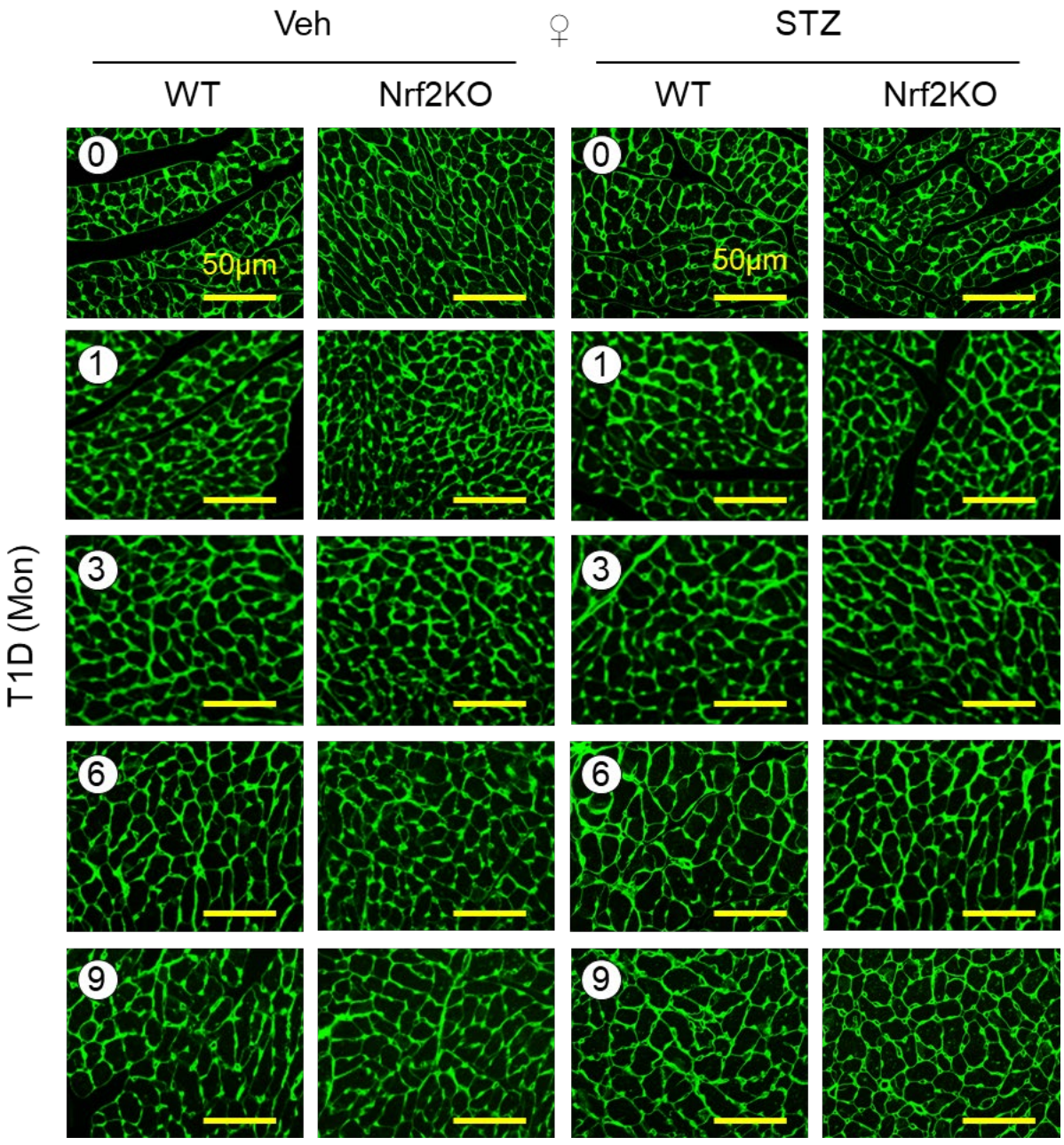

Supplementary Fig. 11. The impact of global knockout of Nrf2 on cardiomyocyte hypertrophy in STZ-induced type 1 diabetic female mice. The results are representative

Wheat Germ Agglutinin (WGA) staining of Supplementary Fig. 10*B* showing cardiomyocyte sizes in the left ventricles (LVs) of female (♀) WT and Nrf2 KO mice at 0, 1, 3, 6, 9 months (Mon) after onset of STZ-induced type 1 diabetes (T1D). Scale bar = 50 μm**.**

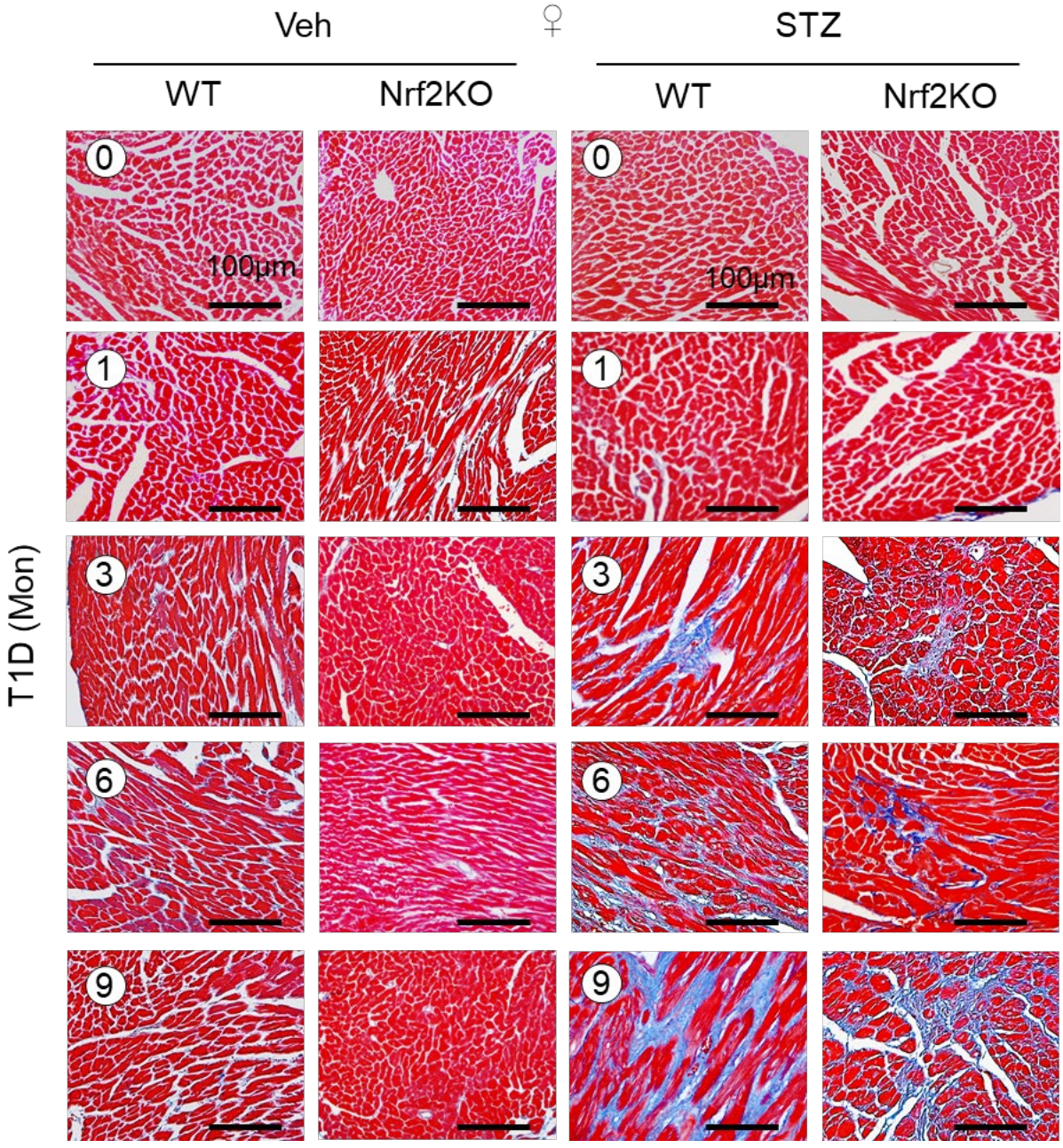

Supplementary Fig. 12. The impact of global knockout of Nrf2 on cardiac fibrosis in STZ-induced type 1 diabetic female mice. The results are representative Masson trichrome staining of Supplementary Fig. 10*C* showing cardiac fibrosis (%) in the left ventricles (LVs) of female (♀) of WT and Nrf2KO mice at 0, 1, 3, 6, 9 months (Mon) after onset of STZ-induced type 1 diabetes (T1D). Scale bar = 100 μm.

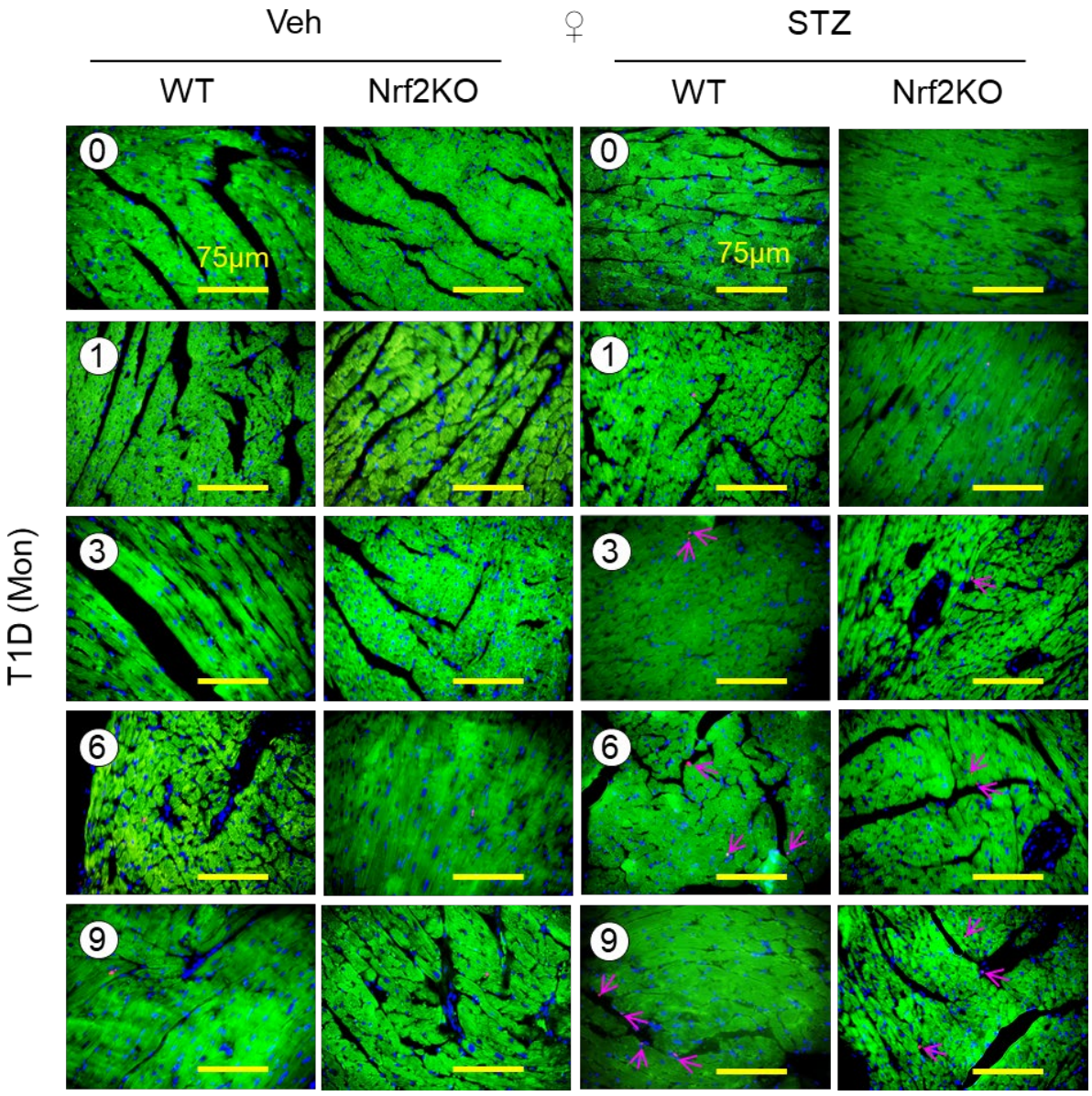

Supplementary Fig. 13. The impact of global knockout of Nrf2 on cardiac apoptosis in STZ-induced type 1 diabetic female mice. The results are representative Tunel staining of Supplementary Fig. 10*D* showing apoptosis (%) in the left ventricles (LVs) of female (♀) WT and Nrf2KO mice at 0, 1, 3, 6, 9 months (Mon) after onset of STZ-induced type 1 diabetes (T1D). Cardiomyocytes (green) were marked by Alexa FluorTM 488 Phalloidin (Invitrogen A12379) binds F-actin. Scale bar = 75 μm.

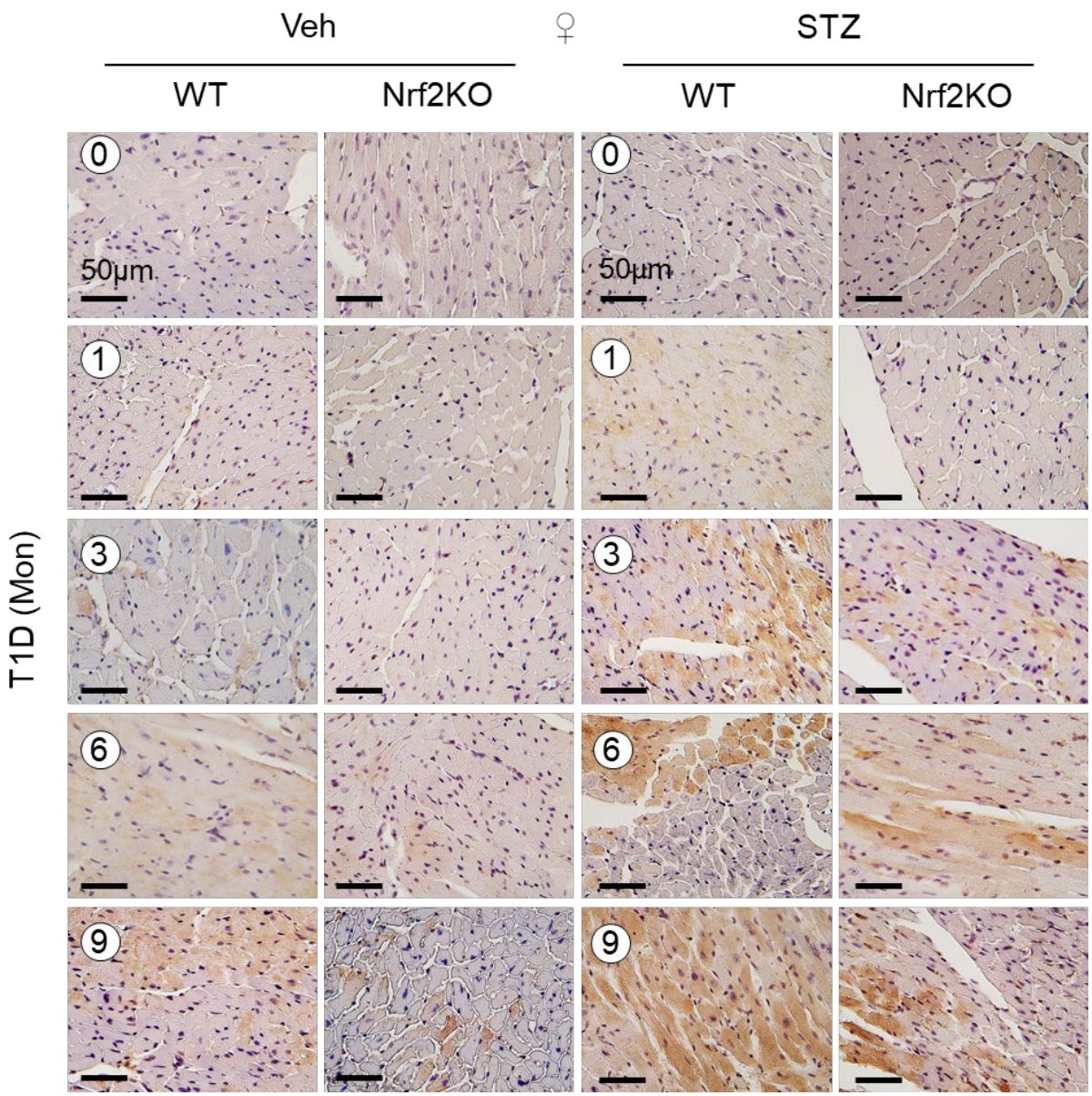

Supplementary Fig. 14. The impact of global knockout of Nrf2 on cardiac lipid peroxidation in STZ-induced type 1 diabetic female mice. The results are representative 4HNE staining of Supplementary Fig. 10*E* showing lipid peroxidation in the left ventricles (LVs) of female (♀) WT and Nrf2KO mice at 0, 1, 3, 6, 9 months (Mon) after onset of STZ-induced type 1 diabetes (T1D). Scale bar = 50 μm.

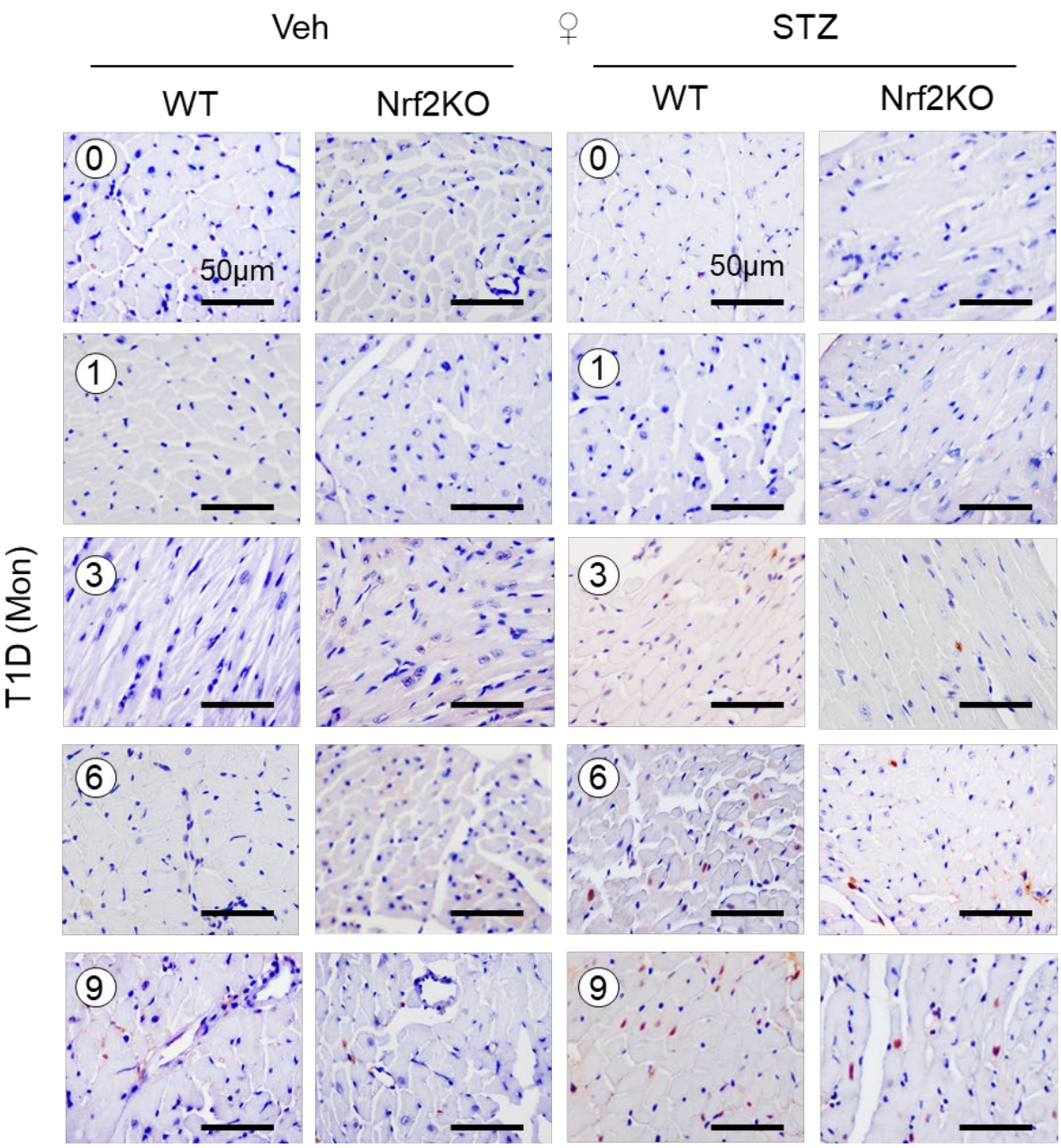

Supplementary Fig. 15. The impact of global knockout of Nrf2 on cardiac oxidative stress-induced DNA damage in STZ-induced type 1 diabetic female mice. The results are representative 8OHdG staining of Supplementary Fig. 10*F* showing oxidative stress-induced DNA damage in the left ventricles (LVs) of female (♀) WT and Nrf2KO mice at 0, 1, 3, 6, 9 months (Mon) after onset of STZ-induced type 1 diabetes (T1D). Scale bar = 50 μm.

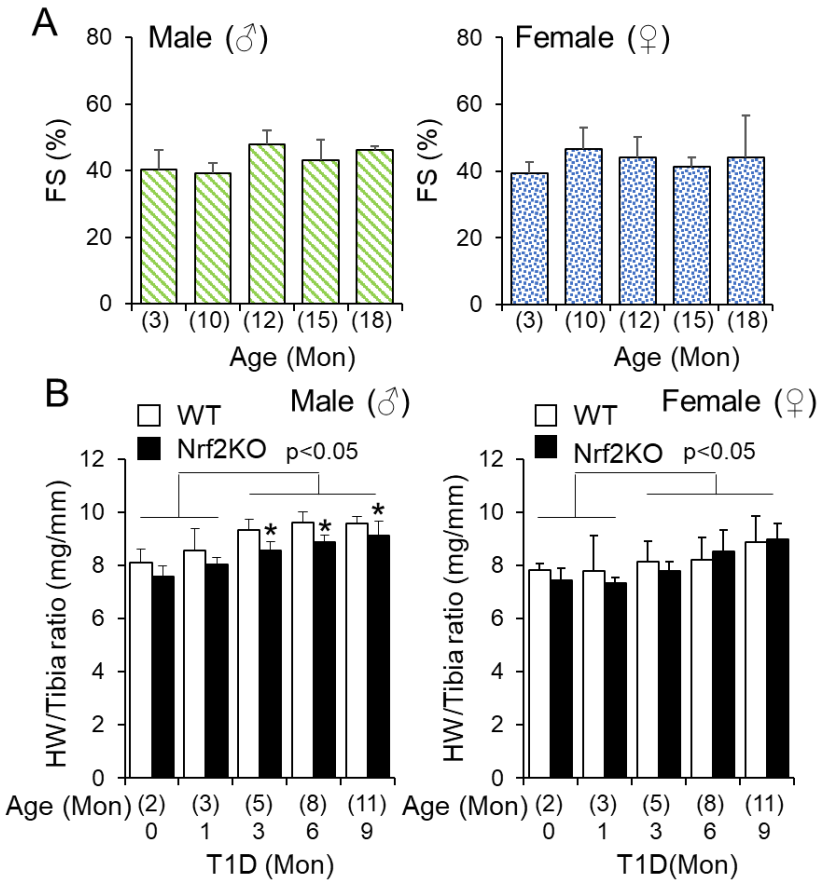

Supplementary Fig. 16. Baseline characterization of cardiac growth and function in WT and Nrf2KO mice during aging. *A*: The impact of aging on cardiac function**.** FS (%) of male (♂) (n=8) and female (♀) (n=6) wild type (WT) FVB/6N mice was monitored up to age of 18 months. *B*: The heart weight (HW)/Tibia length ratio of male and female WT and Nrf2KO mice in a C57BL/6J genetic background was measured from ages of 2 months (Mon) to 11 Mon. n=4~12 in each group, *, $p < 0.05$ vs. WT groups at each time point.

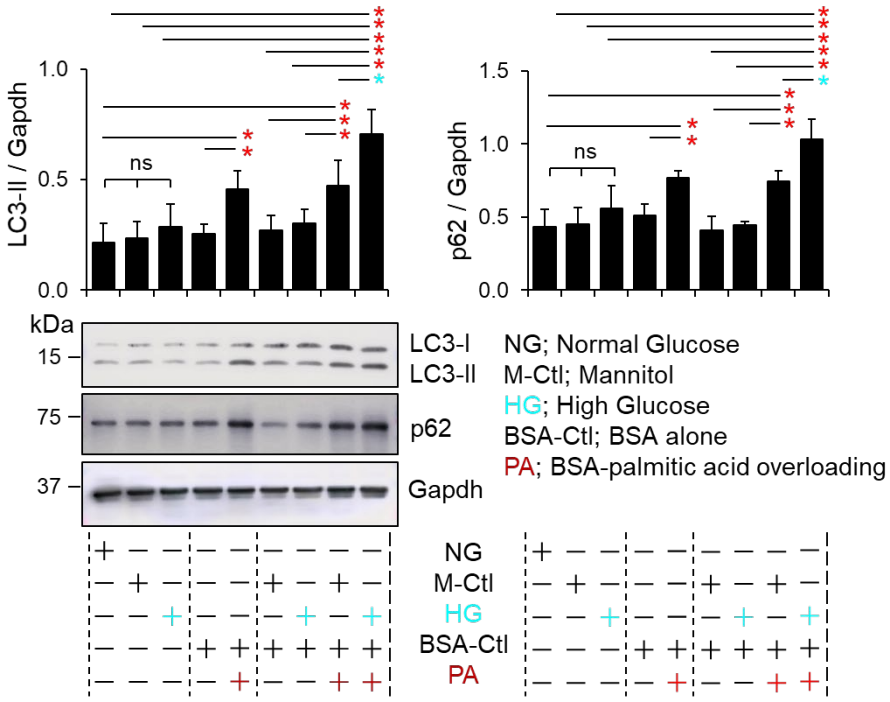

Supplementary Fig. 17. The effects of diabetic settings on LC3 and p62 expression in H9C2 cardiomyocyte-like cells. H9C2 cells were cultured until a confluent state in normal glucose (1 g/L or 5.5 mmol/L) DMEM supplemented 10% FBS and 100 U/ml penicillin and 100 U/ml streptomycin in a 5% CO_2 incubator and then cultured with serum-free normal glucose DMEM (NG), mannitol (30 mmol/L) in normal glucose DMEM (M-Ctl), high glucose (35.5 mmol/L) DMEM, bovine serum albumin (BSA) control, and BSA-palmitic acids (500 µmol/L) as indicated for 24 hours (n=4). The protein expression of LC3 and p62 was assessed by Western blot analysis. *, $p < 0.05$ between indicated groups. ns, non-significant.

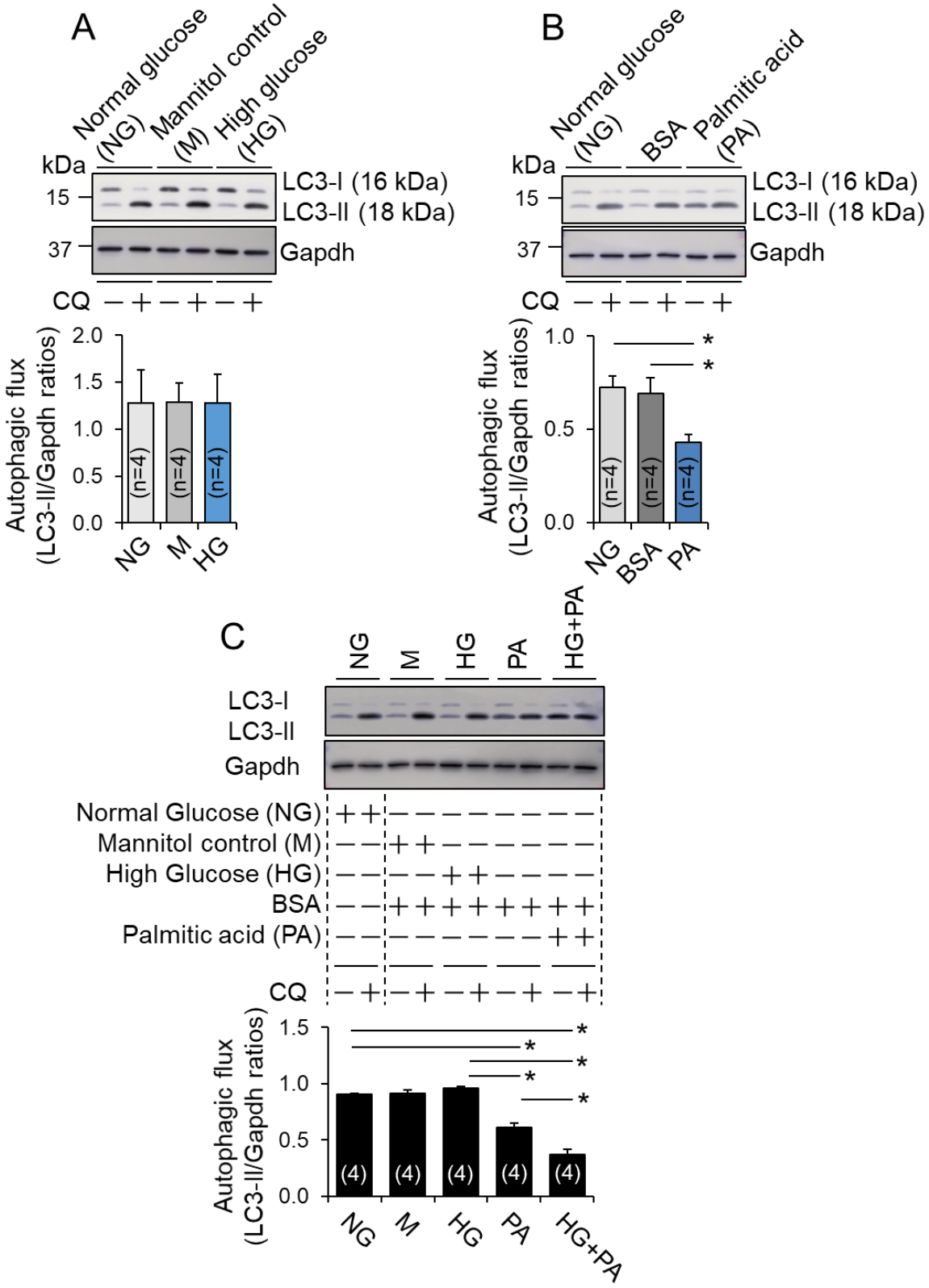

Supplementary Fig. 18. The effects of diabetic settings on autophagy flux in cardiomyocyte-like H9C2 cells. H9C2 were cultured as described in Supplementary Fig. 17 with addition of

chloroquine (CQ, 200 μmol/L) during the last 2 hours of culture (n=4). A: CQ-induced LC3-II accumulation (autophagy flux) in H9C2 cells at a setting of high glucose (HG) milieu. B: CQ-induced autophagy flux in H9C2 cells in a setting of lipid overloading. C: CQ-induced autophagy flux in H9C2 cells in a setting of HG + lipid overloading. *, $p < 0.05$ between indicated groups.

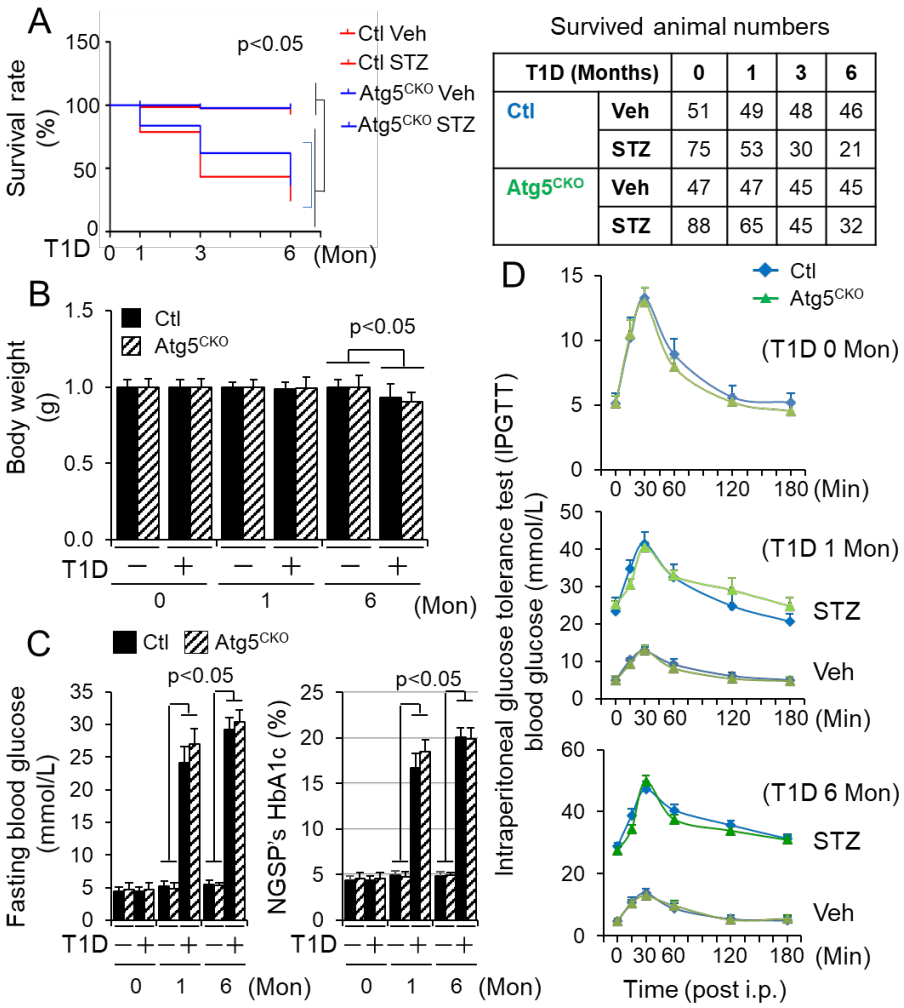

Supplementary Fig. 19. The impact of CR-Atg5KO on STZ-induced diabetes in female mice. Type 1 diabetes (T1D) in littermates of adult female (♀) MerCreMer^{+} control (Ctl) and MerCreMer^{+}::Atg5$^{fl/fl}$ (CR-Atg5KO) mice in a C57BL/6J genetic background after tamoxifen induction was induced by i.p. injection of STZ for 6 months (Mon) as described in Fig. 4*A-B*. *A*: Kaplan Meier analysis of survival rates. *B:* Body weight changes at 0, 1, 6 months after onset of diabetes. *C:* Fasting blood glucose levels and NGSP's HbA1c (%) at 0, 1, 6 months after onset of diabetes. *A-C*: Animal numbers of each group are indicated in the inserted table. *D:* Intraperitoneal injection of glucose tolerance test (IPGTT) was performed at baseline 0, 1, 6 months after onset of diabetes. Three to five animals of each group were randomly selected for the IPGTT.

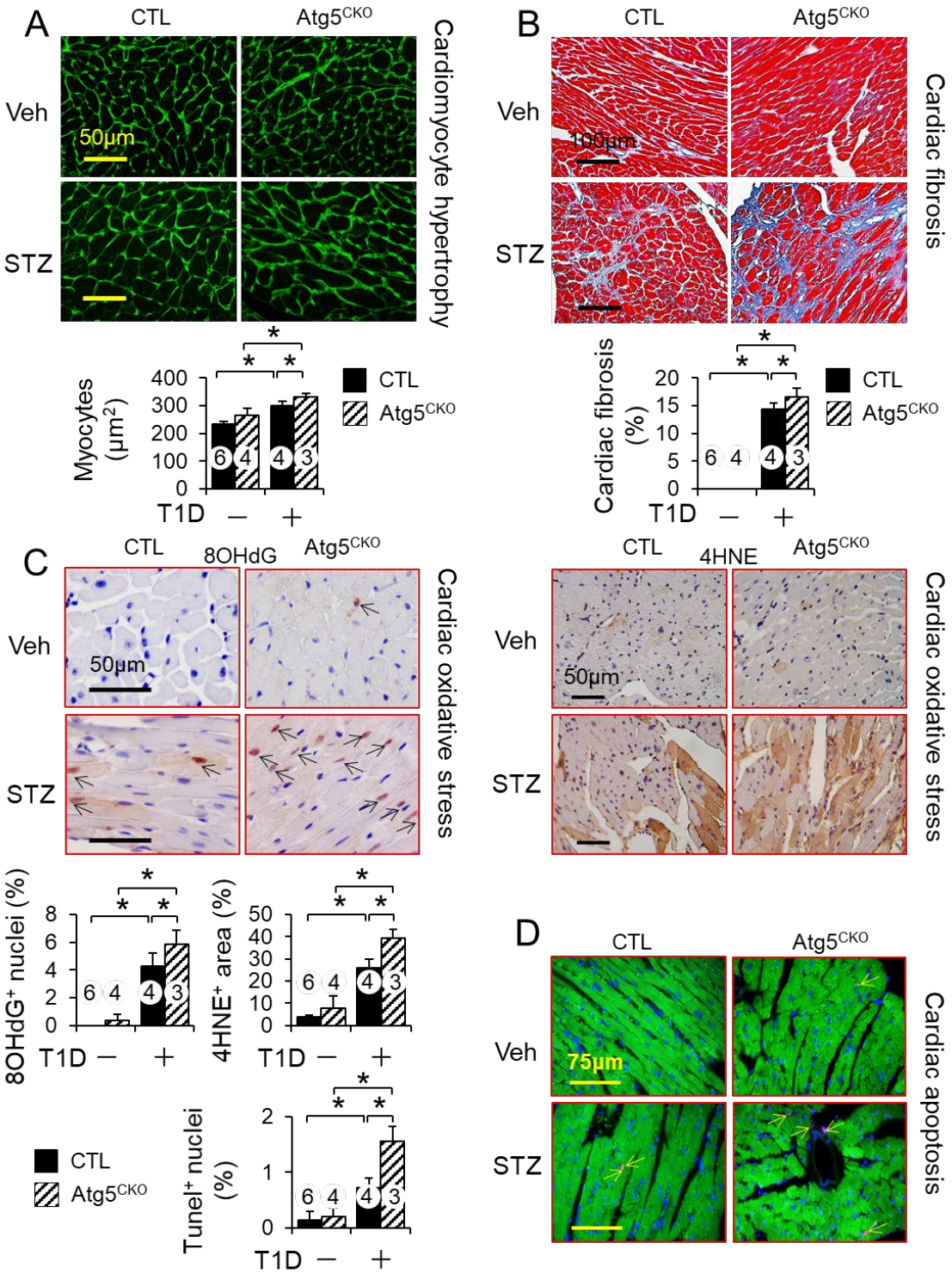

Supplementary Fig. 20. The impact of CR-Atg5KO on cardiac remodeling, cell death and oxidative stress associated with STZ-induced diabetes in female mice. Type 1 diabetes (T1D) in littermates of adult female (♀) MerCreMer^{+} control (Ctl) and MerCreMer^{+}::Atg5$^{fl/fl}$ (CR-Atg5KO) mice was induced by injection of STZ for 6 months as described in Fig. 4*A-B*.

Cardiomyocyte hypertrophy (*A*), cardiac fibrosis (*B*), cardiac oxidative stress (*C*) and cardiac apoptosis (*D*) in left ventricles (LVs) of MerCreMer+ control (CTL) and MerCreMer+::Atg5$^{fl/fl}$ (Atg5^{CKO}) after tamoxifen induction with indicated treatments were analyzed. The results included the representative staining of Fig. 4*B*.

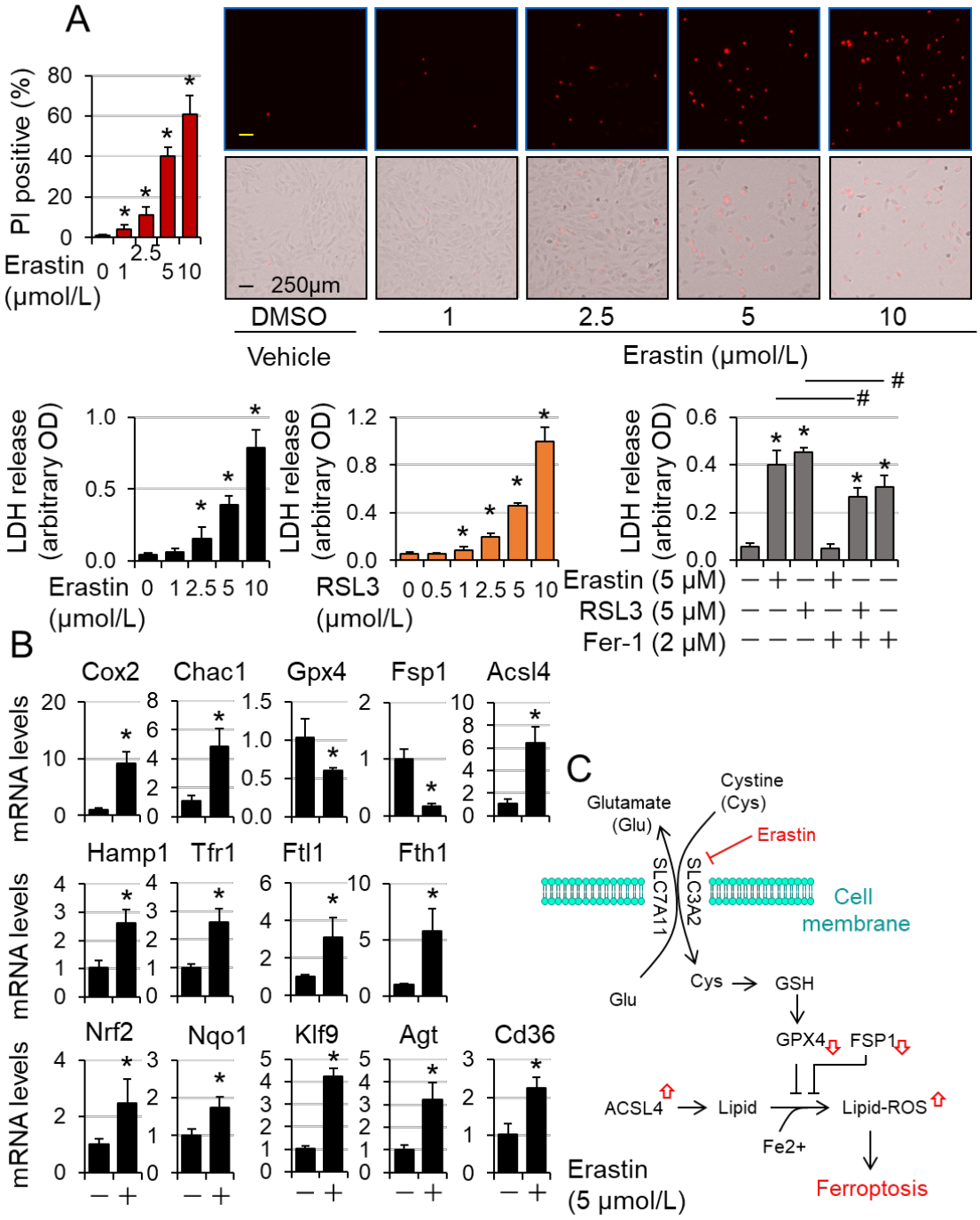

Supplementary Fig. 21. A potential role of Nrf2 in mediating ferroptosis in H9C2 cardiomyocyte-like cells. Sub-confluent H9C2 cells were treated with erastin, RSL3, and ferrostatin-1 (Fer-1) in serum-free DMEM for 24 hours and then were subject to assessments of

cell death or gene expression as indicated. *A*: Cell death. Upper left: Quantified PI positive cells (%). Upper right: The representative propidium iodide (PI) staining. Lower panel shows erastin- or RSL3-induced ferroptosis. n=4, *, $p < 0.05$ between indicated groups. *B*: qPCR analysis of gene expression. n=4, *, $p < 0.05$ between indicated groups. *C*: A scheme of erastin-induced signaling network for driving ferroptosis in H9C2 cardiomyocyte-like cells. Erastin inactivates GPX4, downregulates FSP1, and upregulates ACSL4, thereby promoting lipid peroxidation towards ferroptosis.

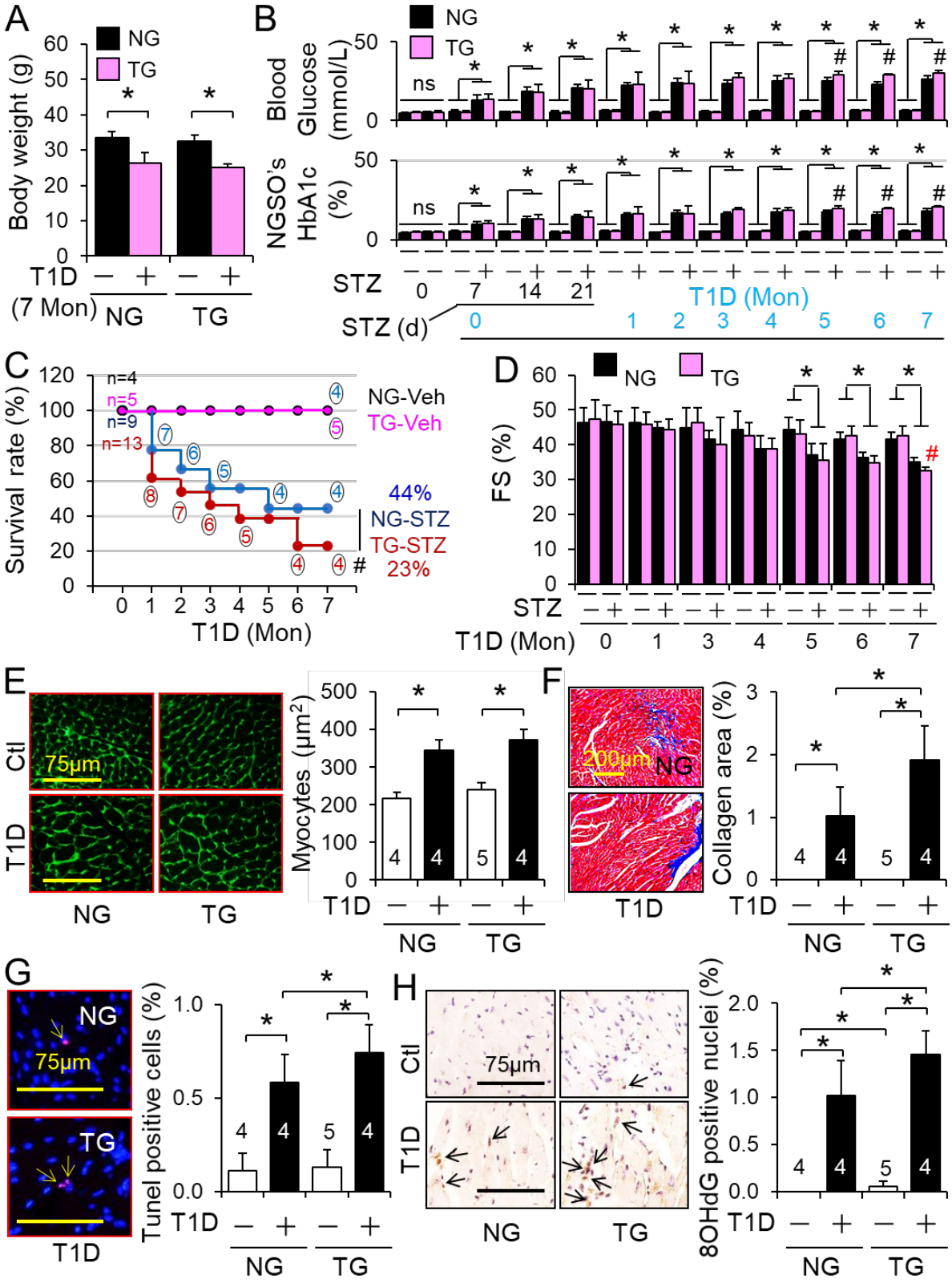

Supplementary Fig. 22. The effect of CR-Nrf2 overexpression on type 1 diabetes-induced cardiomyopathy in female mice. Type 1 diabetes (T1D) in littermates of adult female (♀) non-

transgenic wild type (NG) and CR-Nrf2 transgenic (TG) mice in a FVB/N genetic background was induced by i.p. injection of STZ for 7 months (Mon) and STZ-induced T1D and pathologies were assessed as described in “Research Design and Methods”. *A*: Body weights of NG and TG mice at 7 months after onset of diabetes. *, $p < 0.05$ between indicated groups. *B*: Fasting blood glucose levels and NGSP’s HbA1C (%) of NG and TG mice over a time period of 7-month onset of diabetes. *, $p < 0.05$ between indicated groups; #, $p < 0.05$ vs STZ treated NG at the same time point. *C*: Survival rates. #, $p < 0.05$ vs NG treated with vehicle (Veh). *D*: Cardiac function, FS (%). *, $p < 0.05$ between indicated groups; #, $p < 0.05$ vs STZ treated TG at 7 months. Animal numbers of each experimental groups (*A-D*) are indicated in *C*. *E*: Cardiac myocyte size. *F*: Cardiac fibrosis. *G*: Cardiac apoptosis. *H*: Cardiac oxidative stress. *E-H* in left ventricle (LV) tissue sections of NG and TG mice at 7 months after onset of diabetes were analyzed. Animal numbers of each experimental groups (*E-H*) are indicated in each figure. *, $p < 0.05$ between groups. d; day.

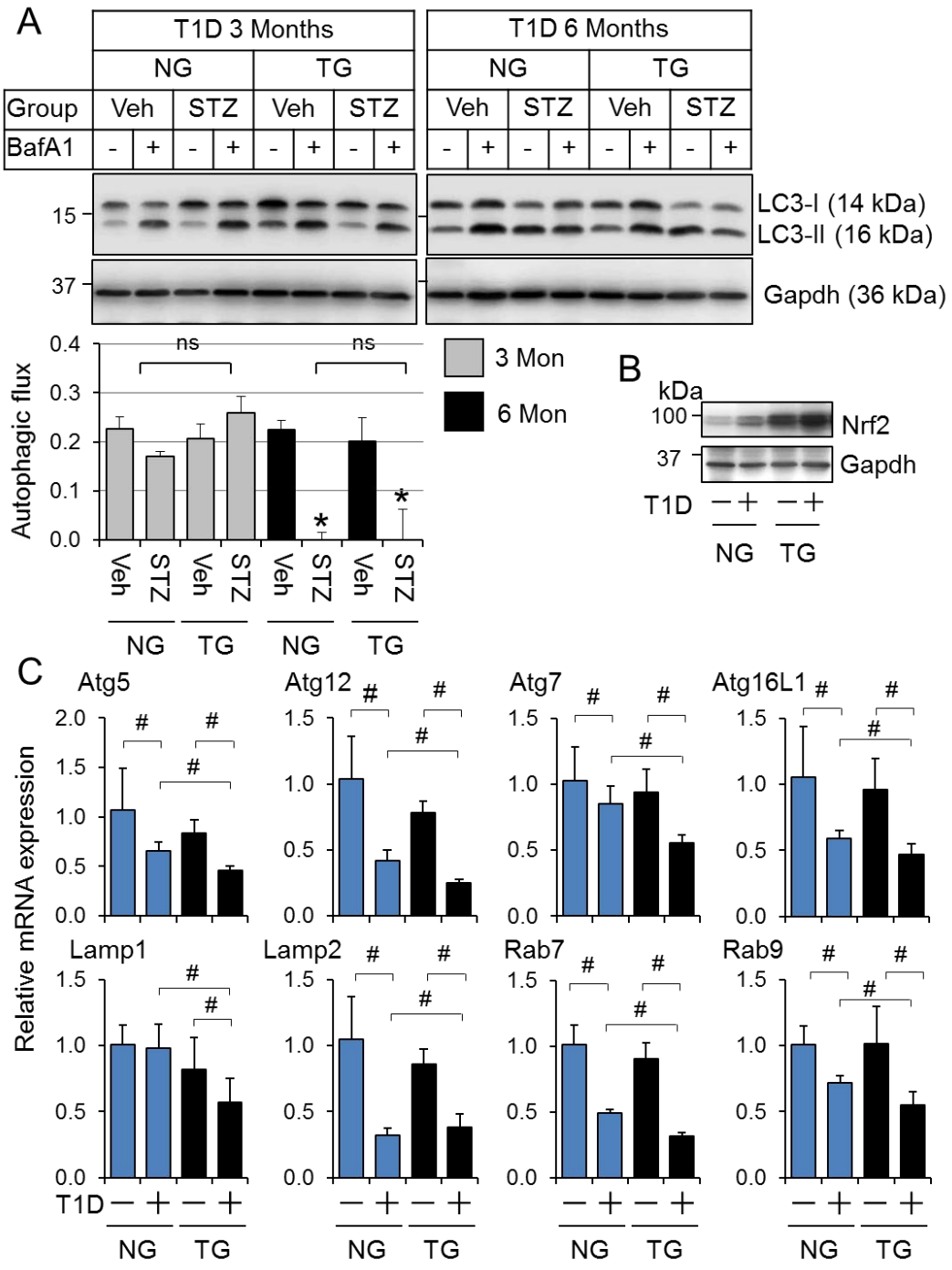

Supplementary Fig. 23. The impact of CR-Nrf2 overexpression on cardiac autophagy in STZ-induced diabetic male mice. Type 1 diabetes (T1D) in littermates of adult male (♂) non-transgenic WT (NG) and CR-Nrf2 Tg (TG) mice in a FVB/N genetic background was induced by i.p. injection of STZ for 6 months (Mon) and then were subject to the assessments of myocardial autophagic flux, and genes or protein expression in left ventricles (LVs) as indicated. *A*: The impact of CR-Nrf2 overexpression on T1D-induced suppression of cardiac autophagic flux in mice. The upper panel is the representative immunoblots and the lower panel is the

autophagic flux (n=4). ns, non-significant; *, $p < 0.05$ vs. Veh controls in the same groups. *B*: Representative immunoblots of Nrf2 protein expression in NG and TG mice. *C*: Relative mRNA expression of autophagy related genes in the heart at 6 months after onset of diabetes. n=4; #, $p < 0.05$ between indicated groups.

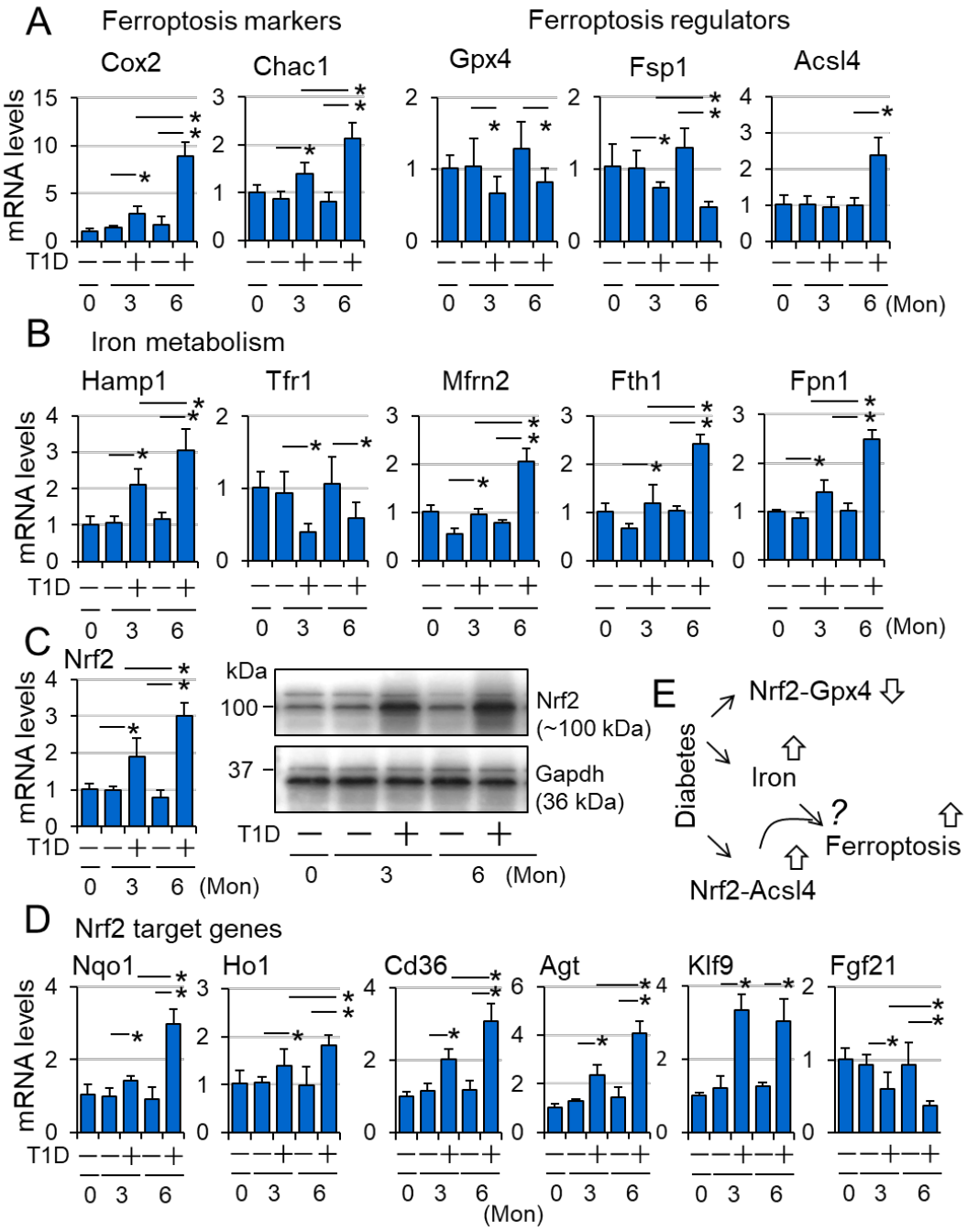

Supplementary Fig. 24. The impact of type 1 diabetes on myocardial Nrf2 signaling in male mice: Potential activation of Nr2-mediated ferroptosis? Type 1 diabetes (T1D) in adult male (♂) wild type mice in a FVB/N genetic background was induced by i.p. injection of STZ for 6 months (Mon) and then were subject to the assessments of myocardial gene or protein expression

as described in “Research Design and Methods”. Left ventricle tissues of the NG and TG mice were used to measure gene and protein expression as follows: *A*: Relative mRNA expression of ferroptosis marker and regulator genes. *B:* Relative mRNA expression of genes regulating iron metabolism. *C*: Nrf2 expression. Left panel shows relative Nrf2 mRNA expression and right panel show Nrf2 protein expression. Representative immunoblotting of Nrf2 protein expression from 4 separated experiments. Western blot analysis was carried out using whole heart tissue lysates. *D*: Relative mRNA expression of typical Nrf2 downstream genes. All results are representatives of several sets of separated experiments (n=4, duplicated qPCR and Western blot analyses). *, $p < 0.05$ between indicated groups. *E*: A working hypothesis. Diabetes over time impairs Nrf2-operating antioxidant defense, such as GPX4 expression and activity, while intensifying Nrf2-driven pathological gene program including ACSL4 expression, thereby activating ferroptosis in the heart.

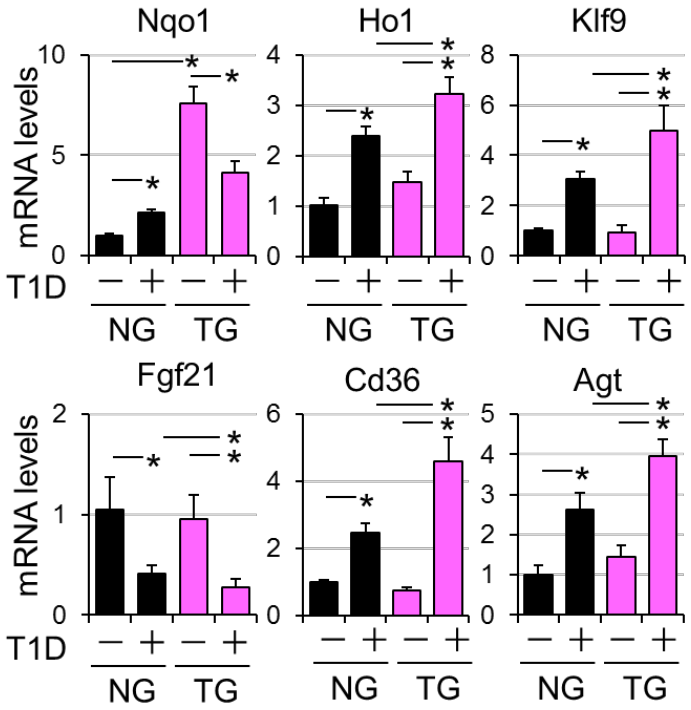

Supplementary Fig. 25. The effect of CR-Nrf2 overexpression on type 1 diabetes-induced dysregulation of myocardial Nrf2 signaling in male mice. Type 1 diabetes (T1D) in littermates of adult male (♂) non-transgenic wild type (NG) and CR-Nrf2 transgenic (TG) mice in a FVB/N genetic background was induced by i.p. injection of STZ for 6 months (Mon) and then were subject to qPCR analysis of myocardial gene expression as described in “Research Design and Methods”. Left ventricles of the NG and TG mice were used to measure gene expression (n=4). *, $p < 0.05$ between indicated groups.